Spin squeezing of a Bose-Einstein condensate via quantum nondemolition measurement for quantum-enhanced atom interferometry

Article (Accepted Version)

Spin Squeezing of a Bose-Einstein Condensate via Quantum Non-Demolition Measurement for Quantum-Enhanced Atom Interferometry

Michail Kritsotakis,[1] Jacob A. Dunningham,[1] and Simon A. Haine[2]

[1] *Department of Physics and Astronomy, University of Sussex, Brighton BN1 9QH, United Kingdom*[*]
[2] *Department of Quantum Science, Research School of Physics and Engineering, The Australian National University, Canberra ACT 2601, Australia*

We theoretically investigate the use of quantum non-demolition measurement to enhance the sensitivity of atom interferometry with Bose-condensed atoms. In particular, we are concerned with enhancing existing high-precision atom interferometry apparatuses, so restrict ourselves to dilute atomic samples, and the use of free-propagating light, or optical cavities in the weak-coupling regime. We find the optimum parameter regime that balances between spin squeezing and atomic loss, and find that significant improvements in sensitivity are possible. Finally, we consider the use of squeezed light, and show that this can provide further boosts to sensitivity.

I. INTRODUCTION

Atom interferometers are powerful tools for making precision measurements particularly in the realm of inertial navigation since they can provide sensitive measurements of accelerations and rotations with very low baseline drift [1, 2]. A lot of interest has therefore developed in finding ways of improving their performance to gain advantage in different applications. It has been shown that Bose-condensed atomic sources can outperform thermal sources due to their narrow momentum linewidth, despite their reduced atomic flux [3–7]. The use of non-classical atomic states such as spin-squeezed states can offset this reduction in flux even further by allowing for sensitivities beyond the shot-noise limit (SNL) [8–11]. In this paper we investigate the use of quantum non-demolition (QND) measurements in collections of Bose-condensed atoms to generate quantum states that could be used to enhance their precision in a range of metrology schemes. The mechanism for generating quantum enhanced many-atom states can be broadly classified into two categories: Those that use atom-atom interactions [9, 12–19], and those that use atom-light interactions [20–38]. While several experiments have demonstrated non-classical states generated through atom-atom interactions [39–48], so far these have been restricted to small numbers of atoms, and have not been applied to atom interferometry capable of inertial measurements. This is partly because the atom-atom interactions required for the generation of the entanglement create unavoidable multimode-dynamics which inhibit mode-matching, [18, 49–52], and phase diffusion [53, 54]. Quantum entanglement through atom-light interactions, which are free to operate in regimes where the effects of atom-atom interactions are negligible, have also been successfully demonstrated. In particular, the use of light to perform QND measurements of the collective atomic spin has shown significant spin-squeezing [55–63]. So far, these experimental demonstrations have been restricted to cold thermal atoms. In this work, we focus on Bose-condensed sources, with the motivation of implementing this quantum enhancement technique on existing high-precision, large space-time area atomic gravimetry setups, such as [64]. In particular, the requirement that the Bose-Einstein condensate (BEC) is expanded before the atomic beam-splitting process dictates a minimum spatial size of the source, and prevents excessively elongated samples such as in [61]. Furthermore, we restrict ourselves to freely propagating light, and find the optimum parameter regime which balances the spin-squeezing and atomic loss caused by spontaneous emission. We also consider the use of optical cavities, but restrict ourselves to cavities that are assembled outside the vacuum chamber, so are inherently low-finesse with weak atom-light coupling due to the large cavity volume. We also consider the use of squeezed light to further enhance the sensitivity.

This paper is structured as follows. In section II we review atom interferometry and quantify how spin-squeezing via QND measurements improves the sensitivity. In section III we introduce a simple model of QND squeezing which allows us to make some simple analytic scaling predictions. In section IV we present our full model including a freely-propagating multimode optical field and decoherence due to spontaneous emission. In section V we derive approximate analytic solutions to this model, and in section VI we analyse the system numerically. In section VII we examine the effect of BEC interactions on the level of spin-squeezing. In section VIII we investigate how the use of squeezed light affects the behaviour. In section IX we investigate the use of an optical cavity.

II. USING QND MEASUREMENTS TO ENHANCE THE SENSITIVITY OF A MACH-ZEHNDER INTERFEROMETER.

Atom interferometers used to measure accelerations and rotations are usually based on the Mach-Zehnder (MZ) configuration [65, 66]. Starting with an ensemble

[*] M.Kritsotakis@sussex.ac.uk

of atoms with two stable ground states, labeled $|1\rangle$ and $|2\rangle$, a $\frac{\pi}{2}$ pulse, or 'beamsplitter', implemented by a two-photon Raman transition is used to place each atom in an equal superposition of these states, while transferring momentum $\hbar\mathbf{k}_0$ to the state $|2\rangle$ component, where $\mathbf{k}_0$ is determined by the difference in wavevectors of the two Raman lasers. The atoms then evolve for a period of time T, before a second Raman transition implements a π pulse, or 'mirror'. After a second period of time T, a second $\frac{\pi}{2}$ beamsplitter pulse is implemented, and the number difference is read-out. Such a system is conveniently described by introducing the pseudo-spin operators $\hat{J}_k$ defined by

$$\hat{J}_k = \frac{1}{2}\left(\hat{a}^\dagger, \hat{b}^\dagger\right)\sigma_k\begin{pmatrix}\hat{a}\\ \hat{b}\end{pmatrix}, \tag{1}$$

with $k = x,\ y,\ z$, where σ_k is the kth Pauli matrix and $\hat{a}$, $\hat{b}$ are the annihilation operators of a particle from $|a\rangle$ and $|b\rangle$ mode respectively. These operators obey the SU(2) commutation relations:

$$\left[\hat{J}_x, \hat{J}_y\right] = i\hat{J}_z,\ \left[\hat{J}_y, \hat{J}_z\right] = i\hat{J}_x,\ \left[\hat{J}_z, \hat{J}_x\right] = i\hat{J}_y\,. \tag{2}$$

It can be shown that the MZ interferometer described above performs the operation

$$\hat{J}_k = e^{i\hat{J}_y\theta}\hat{J}_k(0)e^{-i\hat{J}_y\theta}\,. \tag{3}$$

where θ is the phase difference that has accumulated between the two arms of the interferometer, and $\hat{J}_k(0)$ are the operators before the pulse sequence [7, 67–69]. For a gravimeter, $\theta = \boldsymbol{g}\cdot\mathbf{k}_0T^2$ where $\boldsymbol{g}$ is the gravitational field. The task of estimating g, the magnitude of the gravitational field parallel to $\mathbf{k}_0$ then comes down to our ability to estimate θ. That is, $\Delta g = \Delta\theta/|\mathbf{k}_0|T^2$.

For a particular measurement signal $\hat{S}$, the sensitivity is given by

$$\Delta\theta = \sqrt{\frac{\mathrm{Var}(\hat{S})}{(\partial_\theta\langle\hat{S}\rangle)^2}}\,. \tag{4}$$

Choosing $\hat{S}_1 = \hat{J}_z$ for $\hat{S}$, the number difference at the output of the interferometer, we find

$$\hat{J}_z = \hat{J}_z(0)\cos(\theta) - \hat{J}_x(0)\sin(\theta)\,. \tag{5}$$

Operating around $\theta \approx 0$, we find

$$\Delta\theta = \sqrt{\frac{\mathrm{Var}(\hat{J}_z)}{(\langle\hat{J}_x\rangle)^2}}\,. \tag{6}$$

Choosing an initial state as N_a uncorrelated atoms in an equal superposition of $|1\rangle$ and $|2\rangle$, i.e. a coherent spin state [70],

$$|\Psi\rangle = \left(\frac{1}{\sqrt{2}}\left(\hat{a}^\dagger + \hat{b}^\dagger\right)\right)^{\otimes N_a}|0,0\rangle\,, \tag{7}$$

we find

$$\Delta\theta = \frac{1}{\sqrt{N_a}}\,, \tag{8}$$

which is the shot-noise limit (SNL). This is the best possible sensitivity for any uncorrelated state. That is, any state of the form $|\Psi\rangle = (c_1|1\rangle + c_2|2\rangle)^{\otimes N_a}$. Equation 8 motivates the introduction of the spin-squeezing parameter ξ_s, defined by

$$\xi_s = \sqrt{N_a}\frac{\sqrt{\mathrm{Var}(\hat{S})}}{|\partial_\theta\langle\hat{S}\rangle|} \tag{9}$$

such that

$$\Delta\theta = \frac{\xi_s}{\sqrt{N_a}}\,. \tag{10}$$

The use of input states with quantum correlations such that $\xi_s < 1$ gives sensitivities better than the SNL. We should point out here that we consider a scheme, where the preparation of the entanglement-enhanced state and the interferometer sequence are two completely separate stages of the whole procedure. Essentially, we firstly prepare a spin-squeezed state, which would be used as the input state of the interferometer. This is the reason why, we will explicitly denote in the following that $\theta = 0$ in the atomic variables, which is the point of interest, since in practice, the interferometer is biased to operate around the most sensitive point, which is $\theta = 0$. A state with $\xi_s < 1$ can be achieved by creating atom-atom entanglement, and also by creating entanglement between the atoms and some auxiliary field, such as an optical beam. By measuring both fields together, it is possible to create a signal with reduced fluctuations and therefore increased sensitivity. Specifically, by measuring the combined signal

$$\hat{S}_2 = \hat{J}_z(0) - \hat{J}_z^{\mathrm{inf}} \tag{11}$$

where $\hat{J}_z^{\mathrm{inf}} = G\hat{S}_b$ represents an inference of the population difference, based on measurements of some optical observable $\hat{S}_b$. The constant G is a proportionality factor, which is found by minimizing the variance of the total signal $\mathrm{Var}(\hat{S}_2)$ with respect to G:

$$G = \frac{\mathrm{Cov}\left(\hat{J}_z(0), \hat{S}_b\right)}{\mathrm{Var}(\hat{S}_b)} \tag{12}$$

which gives:

$$\mathrm{Var}(\hat{S}_2) = \mathrm{Var}(\hat{J}_z(0)) - \frac{\mathrm{Cov}^2(\hat{J}_z, \hat{S}_b)}{\mathrm{Var}(\hat{S}_b)} \tag{13}$$

Hence, creating atom-light entanglement and measuring the appropriate light observable in such a way that $\frac{\mathrm{Cov}^2(\hat{J}_z(0),\hat{S}_b)}{\mathrm{Var}(\hat{S}_b)} > 0$, yields a reduced signal variance

$\mathrm{Var}(\hat{S}_2) < \mathrm{Var}(\hat{J}_z(0)) = \mathrm{Var}(\hat{S}_1)$, increasing the sensitivity over purely measuring the population difference between the two interferometer modes. As the optical observables are unaffected by the MZ sequence, which only acts on atomic degrees of freedom, at $\theta = 0$ we have $\Delta\theta = \xi_{s_2}/\sqrt{N_a}$, where

$$\xi_{s_2} = \frac{\sqrt{N_a}\sqrt{\mathrm{Var}(\hat{S}_2)}}{|\langle \hat{J}_x \rangle|}\,. \tag{14}$$

Hence, if we use an atomic state with $\xi_{s_2} < 1$, as the input state of the interferometer that would result in a performance surpassing the SNL ($\Delta\theta < 1/\sqrt{N}$). If the Hamiltonian responsible for the atom-light entanglement commutes with $\hat{J}_z$, then this is an example of a QND measurement, as there is no measurement back-action on the observable being measured. In the next section we model the atom-light interaction, and quantify how the appropriate choice of $\hat{S}_b$ improves the sensitivity.

III. SIMPLE MODEL: SINGLE MODE LIGHT FIELDS

In order to demonstrate how QND squeezing affects the sensitivity, we begin with a simplified model where we make the single mode approximation for both the atomic fields and optical fields. Assuming an ensemble of two-level atoms in the ground motional state of a trapped BEC, with each level interacting with a far-detuned laser beam, as described in figure 1.

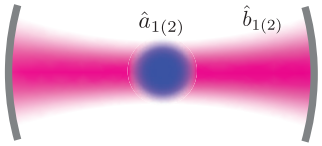

FIG. 1. Simplified scheme showing QND entanglement via an atom-light interaction. An optical mode represented by annihilation operator $\hat{b}_{1(2)}$ interacts with an ensemble of Bose-condensed atoms (annihilation operator $\hat{a}_{1(2)}$).

The simplified Hamiltonian for the system is

$$\hat{H}_{\mathrm{int}} = -\hbar\chi_{\mathrm{sm}}(\hat{a}_1^\dagger\hat{a}_1\hat{b}_1^\dagger\hat{b}_1 + \hat{a}_2^\dagger\hat{a}_2\hat{b}_2^\dagger\hat{b}_2)\,, \tag{15}$$

where χ_{sm} indicates the interaction strength between the atoms and the light in our simple model. Also, $\hat{a}_j = \int u_0^*(\mathbf{r})\hat{\psi}_j(\mathbf{r})\,d^3\mathbf{r}$ annihilates an atom from the ground motional state of the BEC (spatial wavefunction $u_0(\mathbf{r})$), and $\hat{b}_j$ annihilates a photon from the optical mode interacting with atomic state $|j\rangle$. The atomic and light operators satisfy $[\hat{a}_i, \hat{a}_j^\dagger] = \delta_{ij}$ and $[\hat{b}_i, \hat{b}_j^\dagger] = \delta_{ij}$ respectively. As both $\hat{a}_j^\dagger\hat{a}_j$ and $\hat{b}_j^\dagger\hat{b}_j$ commute with the Hamiltonian, the solution to the Heisenberg equations of motion for the system are

$$\hat{a}_j(t) = \hat{a}_j(0)e^{i\chi_{\mathrm{sm}}\hat{b}_j^\dagger(0)\hat{b}_j(0)t} \tag{16a}$$

$$\hat{b}_j(t) = \hat{b}_j(0)e^{i\chi_{\mathrm{sm}}\hat{a}_j^\dagger(0)\hat{a}_j(0)t} \tag{16b}$$

Examining the form of Eq. (16b), we see that the phase of the optical mode is correlated with the population of the corresponding atomic mode. This motivates us to examine $\hat{Y}_{b_j}$, where $\hat{Y}_{b_j} = i\left(\hat{b}_j - \hat{b}_j^\dagger\right)$ is the phase quadrature of the light field. After making the small angle approximation $\chi_{\mathrm{sm}}t\hat{a}_j^\dagger\hat{a}_j << 1$ we find

$$\hat{Y}_j(t) \approx \hat{Y}_{j0} - \chi_{\mathrm{sm}}t\hat{a}_j^\dagger\hat{a}_j\hat{X}_{j0} \tag{17}$$

where $\hat{Y}_{j0} = i(\hat{b}_j(0) - \hat{b}_j^\dagger(0))$ and $\hat{X}_{j0} = \hat{b}_j(0) + \hat{b}_j^\dagger(0)$, and notice that $\hat{Y}_j(t) \propto \hat{N}_{a_j}$. Hence we can make an inference about the atomic population difference by measuring the difference of the two phase quadratures. In order to calculate the strength of these correlations, we choose Glauber coherent states $|\alpha_j\rangle$ and $|\beta_j\rangle$, with $\mathrm{Im}(\alpha_j) = \mathrm{Im}(\beta_j) = 0$ as the initial state for the atomic and optical modes respectively. This corresponds to an atomic state with the expectation value of the spin aligned to the x-axis, but with a fluctuating total number. The choice of a Glauber coherent state rather than a coherent spin state was for computational convenience. It has previously been shown that for large atom number, this state provides almost identical spin-squeezing predictions [71]. As there is no physical process that couples parts of the Hilbert space corresponding to different values of the *total* atom number, whether this state is a true number superposition, or an incoherent mixture of total atom number has no observable consequence [49]. This state can be obtained by beginning with all the atoms in one state, and applying a rotation around the y-axis (i.e. and atomic beamsplitter). Setting $\hat{S}_b = \hat{Y}_2 - \hat{Y}_1$ we find

$$\mathrm{Var}(\hat{S}_b(t)) \approx 2 + 4\chi_{\mathrm{sm}}^2 N_{\mathrm{ph}} N_a t^2\,, \tag{18}$$

and

$$\mathrm{Var}(\hat{S}_2(t)) = \frac{N_a}{4}\left(1 - \frac{2\chi_{\mathrm{sm}}^2 N_a N_{\mathrm{ph}} t^2}{1 + 2\chi_{\mathrm{sm}}^2 N_a N_{\mathrm{ph}} t^2}\right) \tag{19}$$

where $N_{\mathrm{ph}} = |\beta_1|^2 = |\beta_2|^2$ is the expectation value of the number of photons. Using this in Eq. (14) we find

$$\xi_{s_2} = e^{\chi_{\mathrm{sm}}^2 N_{\mathrm{ph}} t^2}\left(1 - \frac{2\chi_{\mathrm{sm}}^2 N_a N_{\mathrm{ph}} t^2}{1 + 2\chi_{\mathrm{sm}}^2 N_a N_{\mathrm{ph}} t^2}\right)^{1/2}\,. \tag{20}$$

We notice in Fig. [2] that we obtain better sensitivities for our signal compared to the SNL, indicating that we have created a spin squeezed state. We find the optimum value for the number of photons $N_{\mathrm{ph}}^{\mathrm{opt}} = \frac{1}{2\chi_{\mathrm{sm}}^2 t^2}$ which gives the minimum value $\left(\xi_{s_2}^{\mathrm{sm}}\right)_{\mathrm{min}} = \sqrt{\frac{e}{N_a}}$.

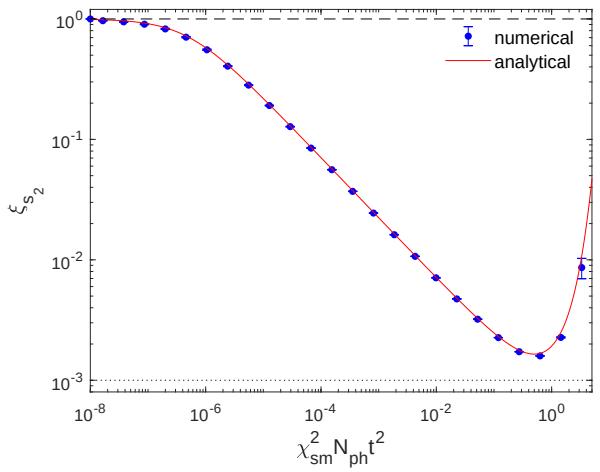

FIG. 2. Simple model: Analytical (solid line) and numerical calculation (dots) of ξ_{s_2} with respect to the collective parameter $\chi^2_{\rm sm} N_{\rm ph} t^2$. The dashed and dotted lines represent the SNL and the Heisenberg limit respectively. The error bars were calculated by taking the standard deviation over many different iterations of the system dynamics.

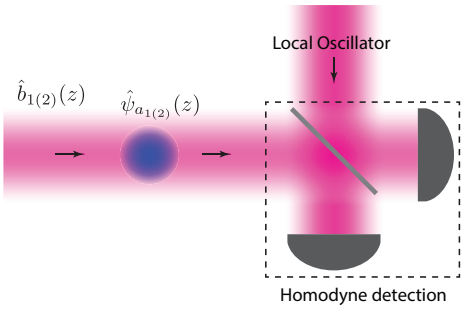

FIG. 3. Schematic of the free-space QND scheme. After interacting with the atomic ensemble, the freely propagating optical field is measured via homodyne detection.

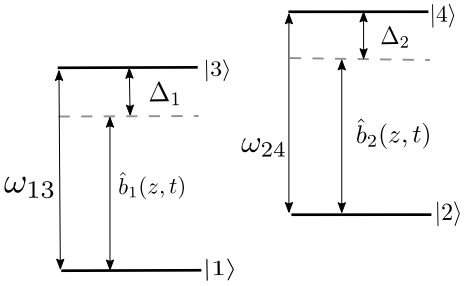

FIG. 4. Atomic energy diagram of the two 2-level systems. Each atom is placed in a superposition of electronic states $|1\rangle$ and $|2\rangle$, with excited states $|3\rangle$ and $|4\rangle$. Two independent lasers (annihilation operator $\hat{b}_1$ and $\hat{b}_2$) are detuned from the $|1\rangle \to |3\rangle$ and $|2\rangle \to |4\rangle$ transitions by detuning Δ_1 and Δ_2, respectively.

This section demonstrates that this kind of atom-light interaction creates an atomic spin squeezed state and consequently boosts the interferometer's performance. In the following section we model the system more rigorously, using the freely propagating light field and including the effects of atomic spontaneous emission.

IV. DETAILED MODEL DESCRIBING ATOM-LIGHT INTERACTION

We now consider a more detailed model that more accurately captures the relevant physics. In particular, in order to model propagating laser beams, we require a multi-mode model for the optical fields (see figure 3). We also include spontaneous emission from the excited atomic states, which will limit the amount of QND squeezing in practice.

A. Equations of motion describing atom-light interaction

We assume an ensemble of Bose-condensed atoms with two electronic states $|1\rangle$ and $|2\rangle$, coupled to excited states $|3\rangle$ and $|4\rangle$ respectively (Fig. 4). The coupling is achieved by far-detuned lasers, which are described by annihilation operators $\hat{b}_1(z,t)$ and $\hat{b}_2(z,t)$, satisfying the commutation relations $[\hat{b}_i(z,t), \hat{b}^\dagger_j(z',t)] = \delta_{ij}\delta(z-z')$ for $i,j = 1,2$. We assume both optical fields have narrow linewidths compared to the natural linewidths of the atomic transitions, with central frequencies given by $\omega_{L_1} = \omega_{13} - \Delta_1$ and $\omega_{L_2} = \omega_{24} - \Delta_2$, where Δ_1 and Δ_2 are the detunings from the $|1\rangle \to |3\rangle$ and $|2\rangle \to |4\rangle$ transitions, respectively. The Hamiltonian for the total system after making the rotational-wave-approximation (RWA) is

$$\begin{aligned}\hat{H}_{\rm tot} = \hbar \int_{-\infty}^{\infty} dz \left(\omega_{13}\hat{\psi}^\dagger_3(z,t)\hat{\psi}_3(z,t) + \omega_{24}\hat{\psi}^\dagger_4(z,t)\hat{\psi}_4(z,t)\right) \\ - i\hbar c \int_{-\infty}^{\infty} \hat{b}^\dagger_1(z,t)\partial_z \hat{b}_1(z,t)dz - i\hbar c \int_{-\infty}^{\infty} \hat{b}^\dagger_2(z,t)\partial_z \hat{b}_2(z,t)dz \\ + \hbar g_{13} \int_{-\infty}^{\infty} \left(\hat{\psi}^\dagger_1(z,t)\hat{\psi}_3(z,t)\hat{b}^\dagger_1(z,t) + \text{h.c}\right) dz \\ + \hbar g_{24} \int_{-\infty}^{\infty} \left(\hat{\psi}^\dagger_2(z,t)\hat{\psi}_4(z,t)\hat{b}^\dagger_2(z,t) + \text{h.c}\right) dz\,,\end{aligned} \tag{21}$$

where $\hat{\psi}_i(z,t)$ is the field operator which annihilates an atom from atomic state $|i\rangle$ at position z, and $g_{13} = \frac{d_{13}}{\hbar}\left(\frac{\hbar\omega_{L_1}}{2\epsilon_0 A}\right)^{1/2}$ and $g_{24} = \frac{d_{24}}{\hbar}\left(\frac{\hbar\omega_{L_2}}{2\epsilon_0 A}\right)^{1/2}$ are the atom-light coupling constant, where $d_{13} = -e\langle 3|\hat{\mathbf{r}}|1\rangle$ and $d_{24} = -e\langle 4|\hat{\mathbf{r}}|2\rangle$ are the dipole moment matrix elements for the atomic transitions $|1\rangle \to |3\rangle$ and $|2\rangle \to |4\rangle$ respectively, A is the transverse quantization area of the light

beam and c is the speed of light.

For simplicity in the following we will present the Heisenberg equations of motion just for one two-level system $\{|1\rangle \to |3\rangle,\ \hat{b}_1(z,t)\}$, since the two systems are de-coupled in the sense that the Heisenberg equations of motion for $|1\rangle \to |3\rangle$ and $|2\rangle \to |4\rangle$ are independent. The corresponding equations hold for the second two-level system $\{|2\rangle \to |4\rangle,\ \hat{b}_2(z,t)\}$ as well.

We incorporate spontaneous emission as a Langevin term in our Heisenberg equation of motion, by coupling the atoms being in their excited state to a reservoir of vacuum electromagnetic modes, which is then traced over, described by the Hamiltonian $\hat{H}_{\rm bath} = \hbar \int_{-\infty}^{\infty} dz \int_{-\infty}^{\infty} d\omega\, \omega\, \hat{d}^\dagger(\omega,z)\hat{d}(\omega,z)$, where $\hat{d}(\omega,z)$ is the continuous in space and frequency annihilation operator of the bath satisfying $[\hat{d}(\omega,z), \hat{d}^\dagger(\omega',z')] = \delta(\omega-\omega')\delta(z-z')$. Hence, the equation of motion for $\hat{\psi}_3(z,t)$ in the presence of this Langevin term [72] is

$$\partial_t \hat{\psi}_3(z,t) = -\frac{i}{\hbar}\left[\hat{\psi}_3(z,t), \hat{H}_{\rm tot}\right] + - \left(\frac{\gamma_3}{2}\hat{\psi}_3(z,t) + \sqrt{\gamma_3}\hat{d}_{1_{\rm in}}(z,t)\right), \quad (22)$$

where γ_3 is the spontaneous emission rate from the excited state and $\hat{d}_{1_{\rm in}}(z,t) = \frac{1}{\sqrt{2\pi}}\int_{-\infty}^{\infty} d\omega e^{-i\omega(t-t_0)}\hat{d}_0(\omega,z)$ is the standard Langevin noise term depending on the value of the bath operator at the initial time point t_0, $\hat{d}(\omega,z,t=t_0) = \hat{d}_0(\omega,z)$. After moving to a rotating reference frame, with respect to the central frequency of the light field, ω_{L_1}, we adiabatically eliminate the excited state field operator $\hat{\psi}_3$, [73]. Thus, the Heisenberg equations of motion for $\hat{\psi}_1(z,t)$ and $\hat{b}_1(z,t)$ are

$$\partial_t \hat{\psi}_1(z,t) = i g_{13}^2 \frac{\Delta_1 + i\frac{\gamma_3}{2}}{\Delta_1^2 + \frac{\gamma_3^2}{4}} \hat{b}_1^\dagger(z,t)\hat{b}_1(z,t)\hat{\psi}_1(z,t) + g_{13}\frac{\sqrt{\gamma_3}}{\Delta_1 - i\frac{\gamma_3}{2}}\hat{b}_1^\dagger(z,t)\hat{d}_{1_{\rm in}}(z,t), \quad (23a)$$

$$\left(\frac{1}{c}\partial_t + \partial_z\right)\hat{b}_1(z,t) = i\frac{g_{13}^2}{c}\frac{\Delta_1 + i\frac{\gamma_3}{2}}{\Delta_1^2 + \frac{\gamma_3^2}{4}}\hat{\psi}_1^\dagger(z,t)\hat{\psi}_1(z,t)\hat{b}_1(z,t) + \frac{g_{13}}{c}\frac{\sqrt{\gamma_3}}{\Delta_1 - i\frac{\gamma_3}{2}}\hat{\psi}_1^\dagger(z,t)\hat{d}_{1_{\rm in}}(z,t). \quad (23b)$$

where Δ_1 is the detuning of the transition from the ground to the excited state. We solve the equation for the light field by making the substitution $z \to z + ct$. As the timescale for the atomic dynamics is much slower than the timescale for the light to cross the atomic sample, we make the approximation that the light moves between two arbitrary points z_B to z_C instantaneously, i.e $\hat{b}^\dagger(z_B,t)\hat{b}(z_B,t) = \hat{b}^\dagger(z_C,t)\hat{b}(z_C,t)$, as long as there is no atom-light interaction in $[z_B, z_C]$. In addition, as our system is a Bose-Einstein condensate, we assume that all the atoms are in the ground motional state of the trap, which allows us to make the single mode approximation $\hat{\psi}_1(z,t) = u_0(z)\hat{a}_1(t)$. Assuming $\int_{z_L}^{z_R}|u_0(z)|^2 dz \approx 1$ for points z_L and z_R sufficiently far to the left and right of the atomic sample respectively, we can write

$$\hat{b}_1(z_R,t) = \hat{b}_{01}(t)e^{i\frac{g_{13}^2}{c}(\Omega+i\Gamma)\hat{a}_1^\dagger(t)\hat{a}_1(t)} + + \frac{g_{13}}{c}\frac{\sqrt{\gamma_3}}{\Delta_1 - i\gamma_3/2}\hat{a}_1^\dagger(t)\hat{q}_{1_{\rm in}}(t) \quad (24)$$

where we have considered the same motional function for the Langevin noise $\hat{d}_{1_{\rm in}}(z,t) = u_0(z)\hat{q}_{1_{\rm in}}(t)$. We have also defined $\hat{b}_{01}(t) = \hat{b}_1(z_L,t)$, and $\Omega \equiv \frac{\Delta_1}{\Delta_1^2+\gamma_3^2/4}$, $\Gamma_3 \equiv \frac{\gamma_3/2}{\Delta_1^2+\gamma_3^2/4}$ for notation simplicity. In order to find a simpler form for the atomic equation, Eq. (23a), we make the approximation that $\hat{b}_1^\dagger(z,t)\hat{b}_1(z,t) \approx \hat{b}_1^\dagger(z_L,t)\hat{b}_1(z_L,t)$, i.e. the number of photons in the mode does not change to a good approximation. Hence, after making the single mode approximation again we obtain:

$$\partial_t \hat{a}_1(t) = i g_{13}^2 (\Omega + i\Gamma)\hat{b}_{01}^\dagger(t)\hat{b}_{01}(t)\hat{a}_1(t) + g_{13}\frac{\sqrt{\gamma_3}}{\Delta_1 - i\frac{\gamma_3}{2}}\hat{b}_{01}^\dagger(t)\hat{q}_{1_{\rm in}}(t). \quad (25)$$

B. Measurement of the Optical Observables

As in section III, we notice that Eq. (24) indicates correlations between the atomic number and the phase of the light. We can define the phase quadrature for our multimode light field by selecting one specific mode. Specifically, we define $\hat{Y}_{\delta_1} = i\left(\hat{\delta}_1 - \hat{\delta}_1^\dagger\right)$ where

$$\hat{\delta}_1 = \int_0^\tau u_{\rm LO}^*(t)\hat{b}_1(z_D,t)dt \quad (26)$$

where z_D is the position of the photo-detector. Also, $u_{\rm LO}(t)$ corresponds to the temporal mode shape of the local oscillator used in the homodyne detection [74], satisfying

$$\int_0^\tau |u_{\rm LO}(t)|^2 dt = c \quad (27)$$

which ensures $[\hat{\delta}_1, \hat{\delta}_1^\dagger] = 1$ and consequently $[\hat{X}_{\delta_1}, \hat{Y}_{\delta_1}] = -2i$, where $\hat{X}_{\delta_1} = \hat{\delta}_1 + \hat{\delta}_1^\dagger$ is the corresponding amplitude quadrature of $\hat{\delta}_1$. The most appropriate choice of local oscillator for this scheme is one with constant intensity with the frequency matched to the carrier frequency of our optical field, i.e.

$$u_{\rm LO}(t) = \sqrt{\frac{c}{\tau}}. \quad (28)$$

V. APPROXIMATE ANALYTIC SOLUTIONS

We can obtain an analytical estimate of the quantum-enhancement parameter, ξ_{s_2}, after making some approx-

imations. Here we briefly present the basic intermediate steps we made in order to find out ξ_{s_2}, with and without spontaneous emission. A much more detailed presentation of these calculations can be found in the Appendices A - C 4. For simplicity we assume that the atom-light interaction strengths as well as the detunings are the same for the two atomic transitions, i.e $g_{13} = g_{24} = g$ and $\Delta_1 = \Delta_2 = \Delta$ respectively. We also consider that initially the atoms and the light fields are in coherent states with the same amplitudes for the two atomic levels $\hat{a}_{1(2)}(0)|\alpha_{1(2)}\rangle = \sqrt{\frac{N_a}{2}}|\alpha_{1(2)}\rangle$ and for the light $\hat{b}_{01}(t)|\beta_1\rangle = \beta_0|\beta_1\rangle$, $\hat{b}_{02}(t)|\beta_2\rangle = \beta_0|\beta_2\rangle$ where we also assume that $\beta_0 = \beta_0^*$.

A. No Spontaneous emission

Ignoring the effect of spontaneous emission (ie, $\gamma_3 = 0$) vastly simplifies the problem and allows easy comparison with the simple single-mode model of section III. In this case, the calculation of the atomic expectation values we are interested in is quite straightforward:

$$\langle \hat{N}_{a_1}(t)\rangle = \frac{N_a}{2}, \qquad \langle \hat{N}^2_{a_1}(t)\rangle = \frac{N_a}{2}\left(1+\frac{N_a}{2}\right) \tag{29}$$

We can also find the phase quadrature operator by making the small angle approximation $\frac{g^2}{c\Delta}\hat{a}_1^\dagger(t)\hat{a}_1(t) << 1$:

$$\hat{Y}_1(\tau) \approx \hat{Y}_{1_{\rm in}}(\tau) - \frac{g^2}{\sqrt{c\tau}\Delta}\hat{a}_1^\dagger(\tau)\hat{a}_1(\tau)\int_0^\tau \left(\hat{b}_{01}(t)+\hat{b}_{01}^\dagger(t)\right)dt \tag{30}$$

where $\hat{Y}_{1_{\rm in}}(\tau) = i\frac{\sqrt{c}}{\sqrt{\tau}}\int_0^\tau \left(\hat{b}_{01}(t)-\hat{b}_{01}^\dagger(t)\right)dt$.

Here we clearly notice that $\hat{Y}_1 \propto \hat{N}_{a_1}$. That supports our choice for the light signal to be $\hat{J}_z^{\rm inf} \propto \hat{S}_b = \hat{Y}_2 - \hat{Y}_1$. Now using Eq. (29) and (30) we can calculate:

$$\mathrm{Var}(\hat{S}_b) \approx 2\mathrm{Var}(\hat{Y}_1(\tau)) \approx 2 + 4\chi^2_{\rm ns}N_aN_{\rm ph} \tag{31}$$

$$\mathrm{Cov}(\hat{J}_z(\tau),\hat{S}_b(\tau)) = \mathrm{Cov}(\hat{S}_b(\tau),\hat{J}_z(\tau)) \approx \chi_{\rm ns}N_a\sqrt{N_{\rm ph}} \tag{32}$$

$$\mathrm{Var}(\hat{S}_2(\tau)) \approx \frac{N_a}{4}\left(1-\frac{\chi^2_{\rm ns}N_{\rm ph}N_a}{\chi^2_{\rm ns}N_{\rm ph}N_a+1/2}\right), \tag{33}$$

where here $N_{\rm ph} = \beta_0^2\tau$. Also, we have defined $\chi_{\rm ns} \equiv \frac{g^2}{c\Delta}$, where the subscript denotes no spontaneous emission. We finally find the quantum-enhancement parameter:

$$\xi^{\rm ns}_{s_2}(\tau) \approx e^{\chi^2_{\rm ns}N_{\rm ph}}\left(1-\frac{\chi^2_{\rm ns}N_{\rm ph}N_a}{\chi^2_{\rm ns}N_{\rm ph}N_a+1/2}\right)^{1/2}. \tag{34}$$

where we used that $\langle \hat{J}_x(t)\rangle \approx \frac{N_a}{2}e^{-\chi^2_{\rm ns}N_{\rm ph}}$ for $\chi^2_{\rm ns}N_{\rm ph} << 1$. By inspection of Eq. (34) we see that the parameters that affect the sensitivity of our signal are the total number of photons $N_{\rm ph}$, the quantization area of the light field A (through g), the detuning Δ, and the total number of atoms N_a. We also notice that we can always increase the sensitivity of our signal by just increasing $\chi_{\rm ns}N_{\rm ph}N_a$ up to a point that the increase of $e^{\chi^2_{\rm ns}N_{\rm ph}}$ becomes dominant. This is essentially the point that $\langle J_x\rangle$ (denominator of Eq. (14)) has decreased so much that the sensitivity starts decaying. Following that strategy we can always achieve better sensitivity than the standard quantum limit (SQL), as seen in Fig.[5]. Here, we find the minimum of $\xi^{\rm ns}_{s_2}$ by taking the derivative with respect to the collective parameter $\nu = \chi^2_{\rm ns}N_{\rm ph}$:

$$(\xi^{\rm ns}_{s_2})_{\rm min} = \sqrt{\frac{e}{N_a}}. \tag{35}$$

We see that the minimum depends on the inverse of the number of atoms, while the optimum number of photons for which we take that minimum is

$$N^{\rm opt}_{\rm ph} = \frac{1}{2\chi^2_{\rm ns}}. \tag{36}$$

B. Spontaneous emission

With the inclusion of spontaneous emission ($\gamma_3 > 0$), the calculation of the atomic expectation values is much more complicated. We begin by ignoring the effect that quantum fluctuation in the optical field has on the spontaneous emission. That is

$$e^{-g^2\Gamma\int_0^t \hat{b}^\dagger(z,t')\hat{b}(z,t')dt'} \approx e^{-g^2\Gamma\beta_0^2 t} \tag{37}$$

such that

$$\langle \hat{N}_{a_1}(t)\rangle \approx \frac{N_a}{2}\epsilon(t) \tag{38}$$

where $\epsilon(t) \equiv e^{-2g^2\Gamma\beta_0^2 t}$ indicates how fast we lose atoms from our system. Following the same strategy as before we find

$$\mathrm{Var}(\hat{S}_b(\tau)) \approx 2 + 4\chi_1^2N_{\rm ph}N_a\overline{\epsilon(\tau)}, \tag{39}$$

$$\begin{aligned}\mathrm{Cov}(\hat{J}_z(\tau),\hat{S}_b(\tau)) &= \mathrm{Cov}(\hat{S}_b(\tau),\hat{J}_z(\tau))\\ &\approx \chi_1\sqrt{N_{\rm ph}}N_a\epsilon(\tau),\end{aligned} \tag{40}$$

and

$$\mathrm{Var}(\hat{S}_2(\tau)) \approx \frac{N_a}{4}\epsilon(\tau)\left(1-\frac{\chi_1^2N_{\rm ph}N_a\epsilon(\tau)}{\chi_1^2N_{\rm ph}N_a\overline{\epsilon(\tau)}+1/2}\right), \tag{41}$$

where we have defined $\chi_1 \equiv \frac{g^2\Omega}{c}$ and $\overline{\epsilon(\tau)} = \frac{1}{\tau}\int_0^\tau \epsilon(t)dt$ which is the time average of the decay. Note that

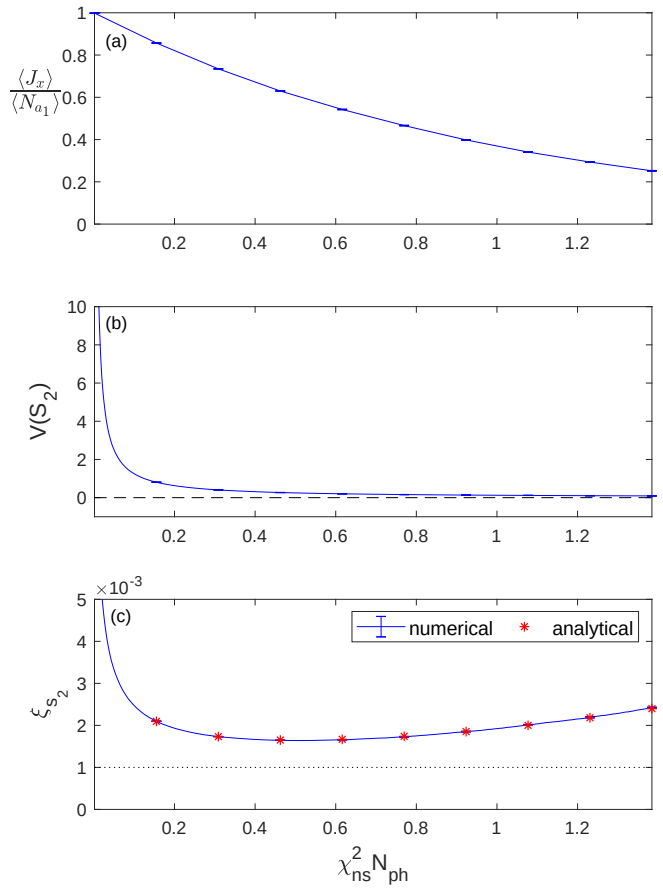

FIG. 5. (a) $\langle J_x\rangle/\langle N_{a_1}\rangle$ (b) $\mathrm{Var}(S_2)$ and (c) ξ_{s_2} with respect to the collective parameter $\nu = \chi^2_{\mathrm{ns}} N_{\mathrm{ph}}$. (a): The decay is due to over-squeezing the state, since we do not consider spontaneous emission here. This causes the squeezing parameter to reach a minimum value (c). The dashed line in (b), points to zero, just to reassure the $\mathrm{Var}(S_2)$ is always positive. In (c) the dotted line represents the Heisenberg limit. The parameter values are $A = 10^{-10}\,\mathrm{m}^2$, $\Delta = 10^2\,\mathrm{GHz}$, $N_a = 10^6$. The error bars are barely distinguishable from all lines.

$\chi_1 = \chi_{\mathrm{ns}}$ in the no spontaneous emission case ($\gamma_3 = 0$). By comparing Eq. (33) with (41) we realise that, except than the apparent effect of particle loss that the atomic spontaneous emission has on the dynamics of the system, there is an additional effect on the variance of the signal, caused by the emergence of the time averaged decay rate in the denominator of Eq. (41), which cannot be reproduced from Eq. (33), by simply making the substitution $N_a \to N_a\epsilon(t)$. Using that $\langle \hat{J}_x(t)\rangle \approx \frac{N_a}{2} e^{-(\chi_1^2+2\chi_2)N_{\mathrm{ph}}}$ for $(\chi_1^2 + 2\chi_2)N_{\mathrm{ph}} << 1$, the spin-squeezing parameter is

$$\xi_{s_2} \approx e^{(\chi_1^2+\chi_2)N_{\mathrm{ph}}} \left(1 - \frac{\chi_1^2 N_{\mathrm{ph}} N_a \epsilon(\tau)}{\chi_1^2 N_{\mathrm{ph}} N_a \overline{\epsilon(\tau)} + 1/2}\right)^{1/2}, \quad (42)$$

where we have defined $\chi_2 \equiv \frac{g^2\Gamma}{c}$ and now the decay factor can be expressed as $\epsilon(\tau) = e^{-2\chi_2 N_{\mathrm{ph}}}$. We also find for the time average of the decay factor that $\overline{\epsilon(\tau)} = \frac{1-\epsilon(\tau)}{2\chi_2 N_{\mathrm{ph}}}$.

By inspecting Eq. (42) it is clear that the case with spontaneous emission is more complicated. We notice again that we can increase the sensitivity by increasing the term $\chi_1^2 N_{\mathrm{ph}} N_a \propto \frac{N_{\mathrm{ph}} N_a}{A^2\Delta^2}$ (for $\Delta >> \gamma_3$), but now we are restricted by the atomic loss rate $\epsilon = \exp(-2\chi_2 N_{\mathrm{ph}}) \propto \exp\left(\frac{N_{\mathrm{ph}}}{A\Delta^2}\right)$ (for $\Delta >> \gamma_3$). Hence, we have to find the appropriate parameter regime that balances between spin squeezing and atomic loss.

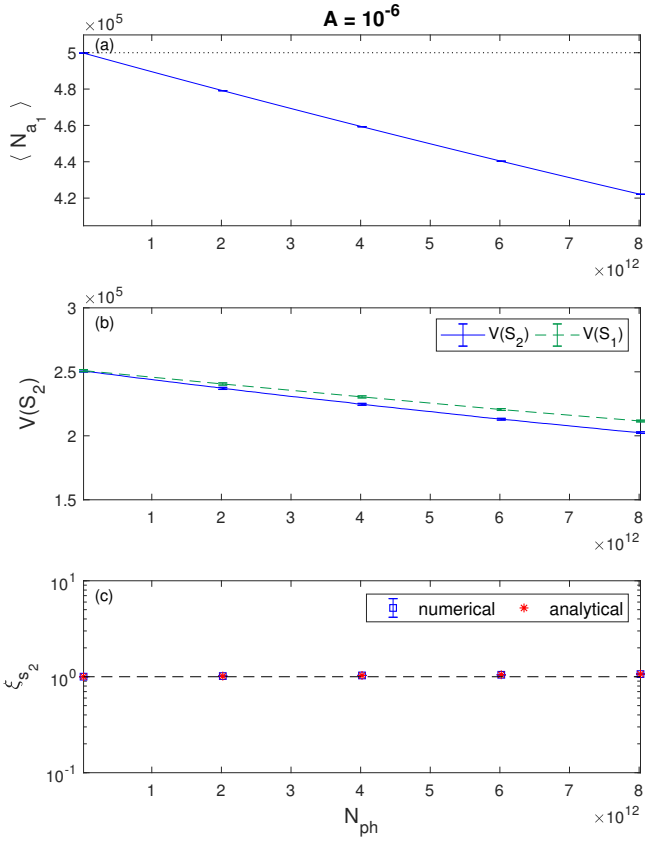

FIG. 6. (a) $\langle N_{a_1}\rangle$, (b) $\mathrm{Var}(S_1)$ (dashed line) and $\mathrm{Var}(S_2)$ (solid line) (c) ξ_{s_2} numerical (squares) and analytical (asterisks) with respect to number of photons. In (a) the dotted line shows the initial atomic population, while the dashed line in (c) represents the SNL. The parameter values are $A = 10^{-6}\,\mathrm{m}^2$, $\Delta = 10^2\,\mathrm{GHz}$, $N_a = 10^6$.

We present simulations of our analytical results for ξ_{s_2}, Fig. [6(c)]-[8(c)], for three different quantization area values, $A = \left(10^{-3}\,\mathrm{m}\right)^2$, $A = \left(10^{-4}\,\mathrm{m}\right)^2$ and $A = \left(10^{-5}\,\mathrm{m}\right)^2$. For each different area value we essentially change the number of photons and detuning appropriately in order to obtain best sensitivities . For $A = \left(10^{-3}\,\mathrm{m}\right)^2$ we no-

tice that we never obtain enhanced sensitivity (compared to SQL) since the loss of atoms exceeds the resulting squeezing, Fig.6 (c). As we decrease A the atom-light interaction strengthens, increasing the sensitivity of our signal Fig.[7,8].

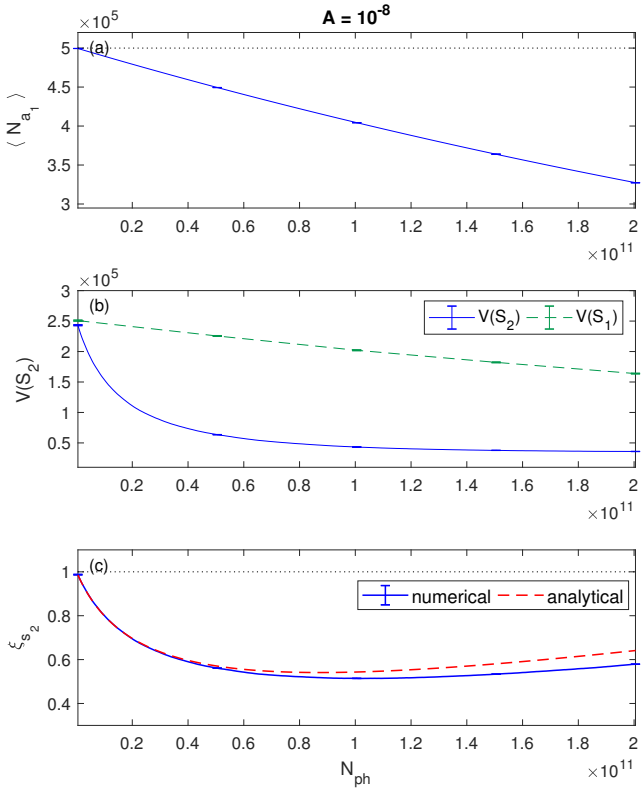

FIG. 7. (a) $\langle N_{a_1}\rangle$, (b) Var(S_1) (dashed line) and Var(S_2) (solid line) (c) ξ_{s_2} numerical (solid line) and analytical (dashed line) with respect to number of photons. In (a) the dotted line shows the initial atomic population, while the black dashed line in (c) represents the SNL. The parameter values are $A = 10^{-8}\,\mathrm{m}^2$, $\Delta = 10^2$GHz, $N_a = 10^6$.

In order to find the minimum of ξ_{s_2}, we express Eq. (42) in terms of the dimensionless parameters $\mu \equiv \frac{\chi_1^2}{\chi_2} = \frac{g^2\Omega^2}{c\Gamma}$, $\lambda \equiv \chi_2 N_{\rm ph}$ and $\zeta \equiv N_a\mu$. Hence, we can now write ξ_{s_2} as

$$\xi_{s_2} = e^{\lambda(1+\mu)}\left(1 - \frac{\zeta\epsilon(\tau)}{\zeta - \zeta\epsilon(\tau) + 1}\right)^{1/2}, \qquad (43)$$

where the decay can now be expressed as $\epsilon(\tau) = e^{-2\lambda}$. We work in a parameter regime where $\mu << 1$, such that

$$\xi_{s_2} \approx e^{\lambda}\left(1 - \frac{2\zeta\lambda e^{-2\lambda}}{1 + \zeta - \zeta e^{-2\lambda}}\right)^{1/2}. \qquad (44)$$

In order to simplify things further, we consider the case where $\Delta >> \gamma_e$. In that case $\Omega \to \frac{1}{\Delta}$ and $\Gamma \to \frac{\gamma_3}{2\Delta^2}$,

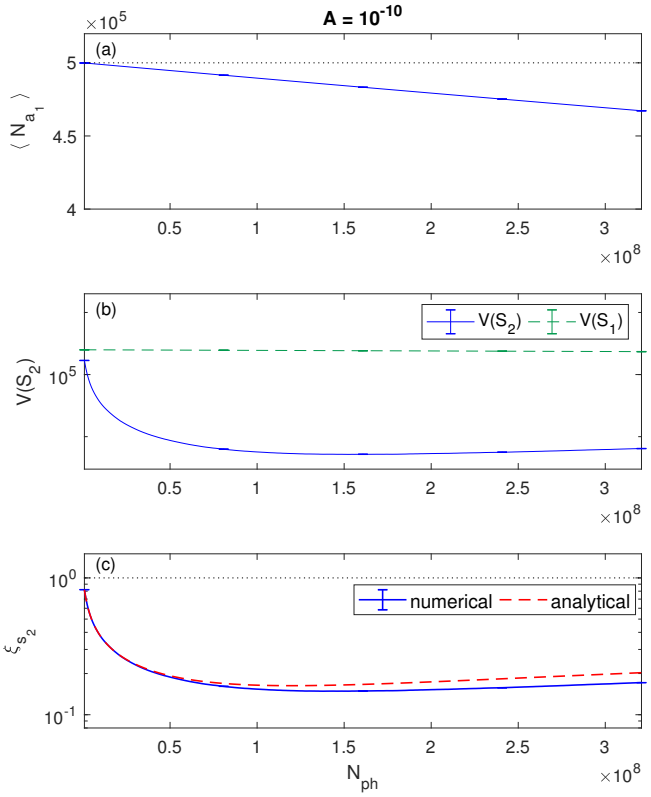

FIG. 8. (a) $\langle N_{a_1}\rangle$, (b) Var(S_1) (dashed line) and Var(S_2) (solid line) (c) ξ_{s_2} numerical (solid line) and analytical (dashed line) with respect to number of photons. In (a) the dotted line shows the initial atomic population, while the dashed line in (c) represents the SNL. The parameter values are $A = 10^{-10}\,\mathrm{m}^2$, $\Delta = 10^2\,\mathrm{GHz}$, $N_a = 10^6$.

thus $\mu \to \frac{2g^2}{c\gamma_3}$. That means that μ only depends on the atomic properties and the quantization area of the light A (through g) and consequently $\zeta \to \frac{2g^2}{c\gamma_3}N_a$. On the other hand $\lambda \to \frac{g^2\gamma_3}{2c}\frac{N_{\rm ph}}{\Delta^2}$ for $\Delta >> \gamma_3$. Hence, if we fix the value of ζ, by choosing a specific value for the number of atoms N_a and the area A, we only need to optimize ξ_{s_2} with respect to λ which is proportional to $N_{\rm ph}/\Delta^2$ in the regime $\Delta >> \gamma_3$. In Fig. [9] we followed that procedure for several different values of ζ and found the minimum of ξ_{s_2} with respect to λ using Eq. (44). We notice that the sensitivity increases as we increase ζ, which means either increasing N_a or decreasing the area. Just to clarify here that by decreasing the area we also increase the atomic loss rate, which leads to loss of sensitivity. In that case we should also change the other parameters $(N_{\rm ph}/\Delta^2)$ in order to counteract that effect, resulting at the end in better sensitivities. On the other hand, the increase of N_a does not affect the loss rate of atoms and it solely improves the sensitivity.

We should mention here that there are similar analyt-

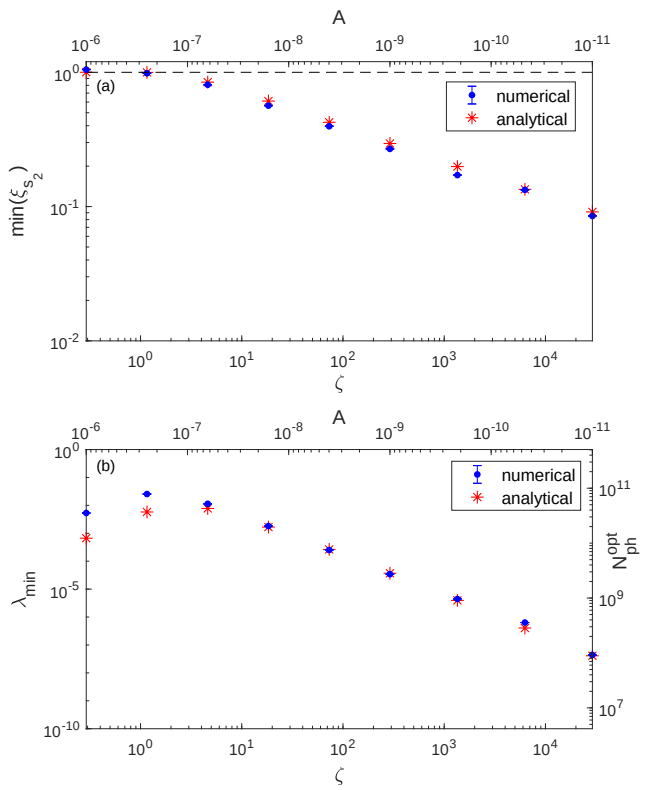

FIG. 9. (a) Minimum value of ξ_{s_2} with respect to ζ (bottom x-axis) and A (top horizontal-axis), (b) optimum λ (left vertical-axis) and optimum number of photons $N_{\rm ph}^{\rm opt}$ (right y-axis) with respect to ζ. In (a) the dashed line represents the SNL.

ical calculations available in the literature [75, 76], but they are limited in the small atomic loss and Gaussian state regime, while our calculations go beyond these assumptions. In the following, we are going to present analytical and numerical results in the case of a phase squeezed light field, as well as numerical calculations including interactions amongst the atoms and the introduction of a cavity, which to our knowledge have not been examined before.

VI. NUMERICAL SOLUTIONS

We can solve for the dynamics of the system numerically by using the Truncated Wigner (TW) method [77]. From the Heisenberg equations of motion we can move to Fokker-Plank equations (FPEs) by using correspondences between quantum operators and Wigner variables. After truncating third and higher order terms we can map the FPEs into stochastic differential equations (SDE) which can be solved numerically with respect to the Wigner variables. We make the following correspondences $\hat{a}_1(t) \rightarrow \alpha_1(t)$, $\hat{b}_1(z,t) \rightarrow \beta_1(z,t)$ and $\hat{q}_{1_{in}}(t) \rightarrow \mathfrak{q}_{in}(t)$. We also consider the initial conditions $\alpha_1(0) = \alpha_{10} + \eta_1$, $\beta_{01}(t) = \beta_0 + w_{b_1}(t)$ and $\mathfrak{q}_{in}(t) = w_{q_1}(t)$. η_1 is complex Gaussian noise satisfying $\overline{\eta_1} = 0$ and $\overline{\eta_1^* \eta_1} = \frac{1}{2}$, $w_x(t)$ is a complex Wiener noise satisfying $\overline{w_x(t)} = 0$ where $x = b_1, q_1$. Also, $\overline{w_{b_1}(t) w_{b_1}(t')} = \frac{1}{2c}\delta(t-t')$ and $\overline{w_{q_1}(t) w_{q_1}(t')} = \frac{1}{2}\delta(t-t')$, where the bar represents averaging with respect to a large number of stochastic trajectories.

We consider the D2 transition line of ^{87}Rb ($5^2S_{1/2} \rightarrow 5^2P_{3/2}$) for both atomic transitions, where the transition frequency is $\omega_{13} = \omega_{24} = \omega_a = 2\pi c/\lambda$ and $\lambda = 780\,$nm. The spontaneous emission rate of the exited state is $\gamma_3 = \gamma_4 = 38.11\,$MHz [78].

More particularly, we numerically examine the SDEs coming from Eq. (24) and (25) for the light and the atoms respectively. For the atomic ensemble of each two level system we consider a single mode field, while for the two light fields we make multi-mode simulations. Our numerical calculations give us the ability to examine the true dynamics of the system, namely we consider the atomic spontaneous emission taking place during the unitary dynamics, which generates the spin squeezing. Most importantly, our numerical method enable us to introduce new features in our system, considering the particle interactions of the two BECs Sec. [VII], as well as examine the cavity case Sec. [IX] and explore how they affect the final sensitivity, by numerically examining the new more complicated dynamics.

In Fig. [6]-[9], we present the numerical simulations corresponding to the analytical results analysed in the previous section. We notice that our analytical and numerical results have almost perfect agreement, indicating that the approximations we made through the derivations do not have any significant effect in the final results.

VII. BEC INTERACTIONS

So far the formalism we have developed could be applied equivalently to both BECs and cold thermal atoms homogeneously coupled to the light field, since essentially the only assumption we have made is that we work under the simple mode approximation for the atomic ensembles of the two 2-level systems. In this section, we examine how interactions amongst the particles of two BECs could affect the dynamics of the QND measurement scheme and how that could change the results we have already presented. We consider that these interactions are described by a Hamiltonian of the form

$$\hat{H}_{\rm BEC}^{\rm int} = \sum_{i,j=1,2} \frac{U_{ij}}{2} \int_{-\infty}^{\infty} \hat{\psi}_i^\dagger(\boldsymbol{r}) \hat{\psi}_j^\dagger(\boldsymbol{r}) \hat{\psi}_i(\boldsymbol{r}) \hat{\psi}_j(\boldsymbol{r})\, dz, \quad (45)$$

where $U_{ij} = \frac{4\pi\hbar^2}{m} a_{ij}$ is the non-linear interaction potential and a_{ij} is the s-wave scattering length between $|i\rangle$ and $|j\rangle$, with $i, j = 1, 2$. In the previous sections we worked under the assumption that the light field propagates only towards the z-axis and hence we could analyse

the dynamics of the atom-light interactions in the 1-D case. However, here that we focus on the interactions amongst the atoms of the two BECs, we develop a 3-D analysis, since we consider that each atomic ensemble forms a sphere of radius $r_{\rm BEC}$. We make the single mode approximation for both BECs, as we did previously

$$\hat{\psi}_1(z,t) = u_{01}(\boldsymbol{r})\hat{a}_1(t), \qquad \hat{\psi}_2(z,t) = u_{02}(\boldsymbol{r})\hat{a}_2(t). \quad (46)$$

Substituting that back in Eq. (45) we obtain

$$\begin{aligned}\hat{H}^{\rm int}_{\rm BEC} =&\hbar\chi_{11}\hat{a}_1^\dagger(t)\hat{a}_1^\dagger(t)\hat{a}_1(t)\hat{a}_1(t) + \hbar\chi_{22}\hat{a}_2^\dagger(t)\hat{a}_2^\dagger(t)\hat{a}_2(t)\hat{a}_2(t)\\ &+ 2\hbar\chi_{12}\hat{a}_1^\dagger(t)\hat{a}_1(t)\hat{a}_2^\dagger(t)\hat{a}_2(t), \quad (47)\end{aligned}$$

where we defined

$$\chi_{ij} = \frac{U_{ij}}{2\hbar}\int_{-\infty}^{\infty}|u_{0i}(\boldsymbol{r})|^2|u_{0j}(\boldsymbol{r})|^2\, d^3\boldsymbol{r}. \quad (48)$$

Alternatively we can use the number density of atoms in order to write

$$\int_{-\infty}^{\infty}|u_{0i}(\boldsymbol{r})|^2|u_{0j}(\boldsymbol{r})|^2\, d^3\boldsymbol{r} = \frac{1}{N_iN_j}\int_{-\infty}^{\infty} n_i(\boldsymbol{r})n_j(\boldsymbol{r})\, d^3\boldsymbol{r}. \quad (49)$$

Assuming constant number density we finally find

$$\chi_{11} = \frac{2\pi\hbar}{mV}a_{11} \qquad \chi_{22} = \frac{2\pi\hbar}{mV}a_{22}, \quad (50)$$

which represents the strength of the intra-particle interactions in each BEC. If we consider that there are no inter-particle interactions, namely the two BECs are separate, then $\chi_{12} = 0$, while if we assume that they are perfectly overlapping then $\chi_{12} = \frac{2\pi\hbar}{mV}a_{12}$. The Hamiltonian in Eq. (47) would add the following terms in the atomic equations of motion for the two 2-level systems

$$\partial_t\hat{a}_1(t) = -2i\left(\chi_{11}\hat{a}_1^\dagger(t)\hat{a}_1(t) + \chi_{12}\hat{a}_2^\dagger(t)\hat{a}_2(t)\right)\hat{a}_1(t) \quad (51)$$

$$\partial_t\hat{a}_2(t) = -2i\left(\chi_{22}\hat{a}_2^\dagger(t)\hat{a}_2(t) + \chi_{12}\hat{a}_1^\dagger(t)\hat{a}_1(t)\right)\hat{a}_2(t). \quad (52)$$

Hence, now we can numerically examine the full dynamics of the system, with the BEC interactions incorporated, using again the TW method. We can essentially do that by transforming the above operator equations of motion into a FPE and map the result to a SDE, as we did earlier. We add the resulted terms in the SDEs of the previous sections, in order to examine the full dynamics. In our simulations we considered the same scattering lengths as in [52, 79], namely $a_{11} = 100.4\,a_0$, $a_{22} = 95.00\,a_0$ and $a_{12} = 97.66\,a_0$, where a_0 is the Bohr radius. We also assumed that the area of the atomic ensemble should be smaller or equal than the transverse area of the light field. In our numerical calculations we used $A_{\rm BEC} = 10^{-11}{\rm m}^2$, corresponding to a radius $r_{\rm BEC} = 2\mu$m for the BEC.

In the previous sections, in the absence of BEC interactions, we noticed that for fixed values of the area (A), the detuning (Δ) and the number of atoms (N_a), we can find the minimum of the squeezing parameter, by adjusting the number of photons. That means that the change of the total time of interaction was equivalent with the change of the light intensity. However, now that we consider interactions amongst the atoms, the time would play a more crucial role in the dynamics, since after some time the atom interactions would become significant resulting in decrease of the final sensitivity. This is shown in Fig. [10(a)], where we notice that considering intra-particle interactions in two separate BECs degrades the sensitivity, while the case of two overlapping BECs perfectly coincides with the no interaction case, since the total interaction strength amongst the atoms is smaller compared to the two separate BECs case. As aforementioned, the number of photons interacting with the atomic ensemble, is what really matters, since it determines the level of squeezing we obtain in the QND measurement scheme. Hence, we can easily find an appropriate regime, in order to avoid the deleterious effects of atom interactions to the final sensitivity, by increasing the light intensity and appropriately decreasing the total interaction time. In that way, we consider the same number of photons, offering the same level of spin squeezing, while everything happens faster, which means that there is not enough time for the atom interactions to damage the final sensitivity, as shown in Fig. [10(b)].

VIII. SQUEEZED LIGHT

Up to this point we have only considered classical light sources. That is, we have assumed that the incoming light is a coherent state, with ${\rm Var}(\hat{Y}_{1_{\rm in}}) = 1$. It is possible to increase the sensitivity of our final signal by considering a squeezed incoming light, where ${\rm Var}(\hat{Y}_{1_{\rm in}})_{\rm sq} = e^{-2r}$ and r is the squeezing factor [74]. In that case our analytical calculation for the spontaneous emission case results in

$${\rm Var}(\hat{S}_b)_{\rm sq} \approx 2{\rm Var}(\hat{Y}_1(\tau))_{\rm sq} \approx 2e^{-2r} + 4\chi_{\rm ns}^2 N_a N_{\rm ph} \quad (53)$$

while the covariances remain the same. Hence, the quantum enhancement parameter become

$$\xi_{s_2} \approx e^{(\chi_1^2+\chi_2)N_{\rm ph}}\left(1 - \frac{\chi_1^2 N_{\rm ph}N_a\epsilon(\tau)}{\chi_1^2 N_{\rm ph}N_a\overline{\epsilon(\tau)} + e^{-2r}/2}\right)^{1/2}. \quad (54)$$

In Fig. [11] we notice that we obtain better sensitivity for all three area values compared to the coherent incident light (Fig. [6 - 8]). In Fig. [12] we show the numerical and analytical $\min(\xi_{s_2})$ for the three different area values, with respect to the degree of optical squeezing in the

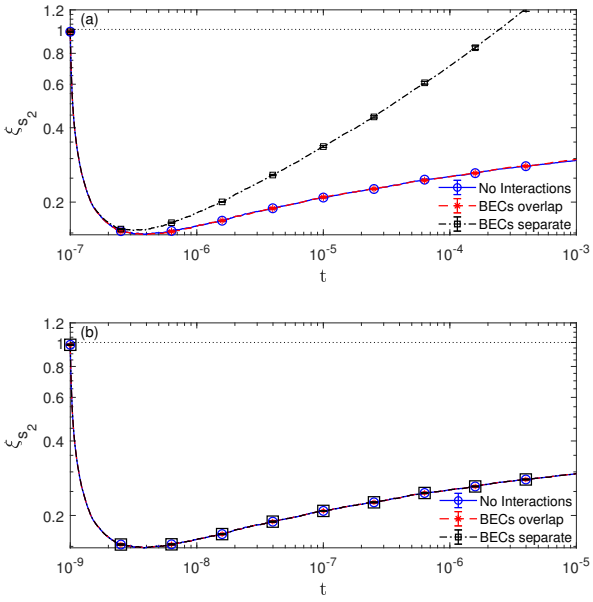

FIG. 10. ξ_{s_2} with respect to time considering three different cases, (i) no atom interactions (solid line with open circles), (ii) atom interactions where the two BECs perfectly overlap (dashed line with asterisks) and (iii) atom interactions, where the two BECs are separate (dash-dotted line with squares). In (a) we consider smaller light intensity and larger total interaction time compared to (b), i.e. in (a) we have $\beta_0^2 = 10^{12}$ photons/s and $\tau = 1$ms, while in (b) $\beta_0^2 = 10^{14}$ photons/s and $\tau = 0.01$ms. The other parameter values are: $N_a = 10^6$, $\Delta = 10^{11}$, $A = 10^{-10}\text{m}^2$, $A_{\text{BEC}} = 10^{-11}\text{m}^2$. The dotted line denotes the SNL.

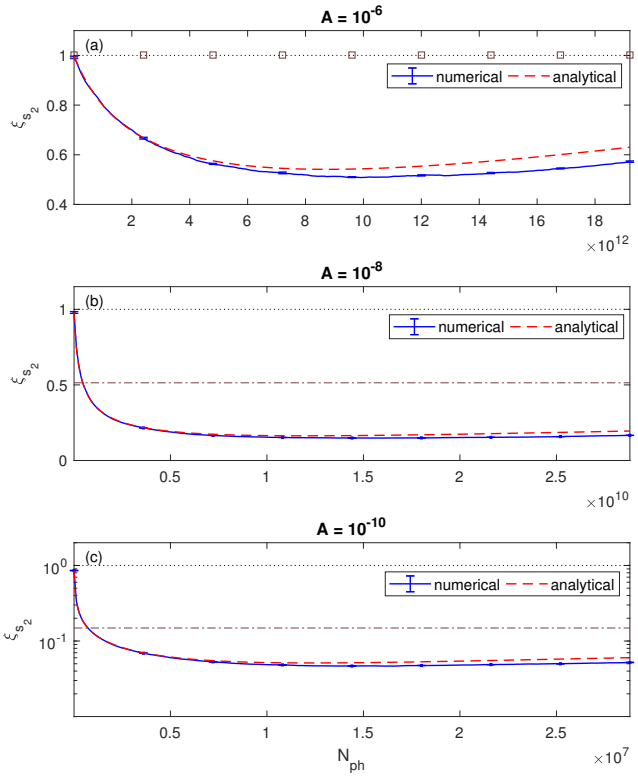

FIG. 11. We consider squeezed incoming light and we examine the numerical (solid line) and analytical (dashed line) evolution of ξ_{s_2} with respect to the number of photons for all three area values. The squares in (a) and dash-dotted lines in (b) and (c) show the $\min(\xi_{s_2})$ of the corresponding cases in Fig. [6] - [8]. The dotted lines denote the SNL. The other parameter values are $r = \ln 10$, $\Delta = 10^2$ GHz, $N_a = 10^6$.

incoming light, $\mathcal{S}$, defined by

$$\mathcal{S} = 10 \log \left(\frac{\sqrt{\text{Var}(\tilde{Y}_{b_1})}}{\sqrt{\text{Var}(Y_{b_1})}} \right) \text{dB}\,, \tag{55}$$

where $\text{Var}(Y_{b_1}) = 1$ is the variance for a coherent state, and $\text{Var}(\tilde{Y}_{b_1}) = e^{-2r}$, where r is the squeezing factor. Using squeezed incoming light gives an exponential rate of decrease for ξ_s for all cases (for $A = 10^{-6}$ that holds for $\gtrapprox$ 5dB). In addition, for a light field with improvement $\gtrapprox$ 5dB we see that we can surpass the SNL even for the $A = 10^{-6}\text{m}^2$ case, while that was impossible when we used a coherent initial state for the light field, Fig. [6] (c). Finally, we notice in Fig [12] that our analytical approximative model (red stars) given by Eq. (54) agrees well with our numerical results (blue circles).

IX. CAVITY DYNAMICS

We can further boost the sensitivity of our signal with the addition of an optical cavity, as it essentially increases the atom-light coupling Fig. [13]. We consider a dual-frequency cavity with resonant frequencies ω_{c_1} and ω_{c_2} detuned from the two atomic transitions $|1\rangle \to |3\rangle$ and $|2\rangle \to |4\rangle$ by detunings Δ_1 and Δ_2 respectively. In the Hamiltonian of our system, Eq. (21) we interchange the continuous light field annihilation operators $\hat{b}_1(z,t)$ and $\hat{b}_2(z,t)$ with the cavity mode annihilation operator $\hat{c}_1$ and $\hat{c}_2$, giving

$$\begin{aligned}\hat{H}^c_{\text{tot}} &= \hbar\omega_{c_1}\hat{c}_1^\dagger\hat{c}_1 + \hbar\omega_{c_2}\hat{c}_2^\dagger\hat{c}_2 \\ &+ \hbar\int_{-\infty}^{\infty} dz \left(\omega_{13}\hat{\psi}_3^\dagger(z,t)\hat{\psi}_3(z,t) + \omega_{24}\hat{\psi}_4^\dagger(z,t)\hat{\psi}_4(z,t)\right) \\ &+ \hbar g_{c_1}\int_{-\infty}^{\infty}\left(\hat{\psi}_1^\dagger(z,t)\hat{\psi}_3(z,t)\hat{c}_1^\dagger(t) + \text{h.c}\right) dz \\ &+ \hbar g_{c_2}\int_{-\infty}^{\infty}\left(\hat{\psi}_2^\dagger(z,t)\hat{\psi}_4(z,t)\hat{c}_2^\dagger(t) + \text{h.c}\right) dz \end{aligned} \tag{56}$$

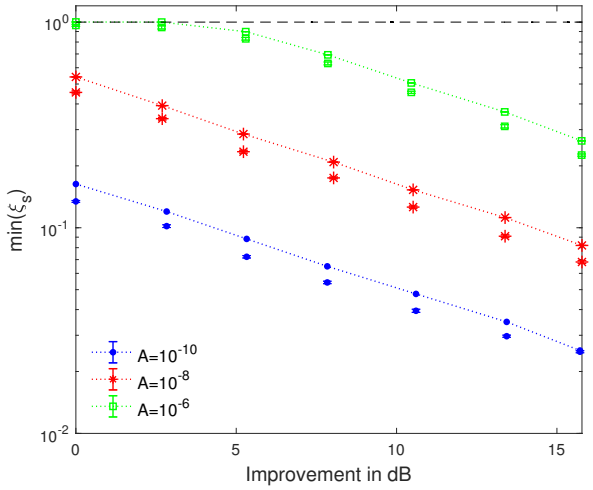

FIG. 12. Analytical (dotted lines with markers) and numerical (markers) calculation of the minimum value of ξ_{s_2} with respect to the improvement in dB of the incoming light field, for the three different area values. The dashed line represents the SNL. The other parameter values are $\Delta = 10^2$ GHz, $N_a = 10^6$.

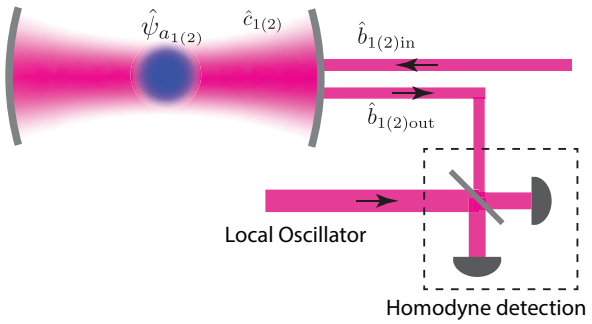

FIG. 13. QND interaction boosted by an optical cavity. After interacting with the atomic ensemble, the light exiting the cavity $\hat{b}_{1(2)\text{out}}$ is measured via homodyne detection.

The coupling strength constants are defined as $g_{c_1} = \frac{d_{13}}{\hbar}\left(\frac{\hbar\omega_{c_1}}{2\epsilon_0 V}\right)^{1/2}$ and $g_{c_2} = \frac{d_{24}}{\hbar}\left(\frac{\hbar\omega_{c_2}}{2\epsilon_0 V}\right)^{1/2}$ where $V = AL$ is the volume of the cavity, A is the light quantization transverse area and L is the cavity length. Using the standard input output formalism [80] we obtain the equation of motion for $\hat{c}_1$

$$\partial_t \hat{c}_1 = -\frac{i}{\hbar}\left[\hat{c}_1, \hat{H}^c_{\text{tot}}\right] - \frac{\kappa}{2}\hat{c}_1 + \sqrt{\kappa}\hat{b}_{1_{\text{in}}}(t)\,, \tag{57}$$

where κ is the cavity photon decay rate, and $\hat{b}_{1_{\text{in}}}(t) = \sqrt{c}\hat{b}_1(z_L, t)$ where c is the speed of light and $\hat{b}_1(z_L, t)$ is the continuous in space annihilation operator of the incoming light field used in the previous sections, satisfying $[\hat{b}_{1_{\text{in}}}(t), \hat{b}_{1_{\text{in}}}(t')] = \delta(t - t')$. Another important quantity is the light field leaking out of the cavity

$$\hat{b}_{1_{\text{out}}}(t) = \sqrt{\kappa}\hat{c}_1(t) - \hat{b}_{1_{\text{in}}}(t)\,. \tag{58}$$

In this case, $\hat{b}_{1_{\text{in}}}(t)$ is an input light field that coherently drives the dynamics of the cavity, but now the mode of the cavity, $\hat{c}_1$, is the one that interacts with the atomic ensemble and is entangled with the atomic ground-state number operator. Again, we incorporate spontaneous emission following the same method as in Sec. (IV), i.e we use Eq. (22) in order to eliminate $\hat{\psi}_3(z,t)$ from the equations of motion for $\hat{\psi}_1(z,t)$ and $\hat{c}_1$. After making the single mode approximation for $\hat{\psi}_1(z,t)$ and $\hat{d}_{1_{\text{in}}}(z,t)$ using again the same mode functions for both of them, and moving to a rotating frame with respect to the cavity resonance frequency we obtain

$$\begin{aligned}\partial_t \hat{a}_1(t) = {} & ig^2(\Omega + i\Gamma)\tilde{c}_1^\dagger(t)\tilde{c}_1(t)\hat{a}_1(t) + \\ & + g_c\frac{\sqrt{\gamma_3}}{\Delta_1 - i\gamma_3/2}\tilde{c}_1^\dagger(t)\tilde{q}_{1_{\text{in}}}(t)\end{aligned} \tag{59a}$$

$$\begin{aligned}\partial_t \tilde{c}_1(t) = {} & \left[ig^2(\Omega + i\Gamma)\hat{a}_1^\dagger\hat{a}_1 - \frac{\kappa}{2}\right]\tilde{c}_1(t) + \\ & + g_c\frac{\sqrt{\gamma_3}}{\Delta_1 - i\gamma_3/2}\hat{a}_1^\dagger(t)\tilde{q}_{1_{\text{in}}}(t) + \sqrt{\kappa}\,\tilde{b}_{1_{\text{in}}}(t)\end{aligned} \tag{59b}$$

where $\tilde{c}_1(t) = \hat{c}(t)e^{i\omega_{c_1}t}$, $\tilde{b}_{1_{\text{in}}}(t) = \hat{b}_{1_{\text{in}}}(t)e^{i\omega_{c_1}t}$, $\tilde{q}_{1_{\text{in}}}(t) = \hat{q}_{1_{\text{in}}}(t)e^{i\omega_{c_1}t}$.

To investigate the dynamics, we use the TW method, again making the appropriate correspondences, in order to numerically examine the dynamics of our system. In Fig. [14] we plot the time evolution of the number of atoms and the number of cavity photons as well as the intensity of the input and output fields. We see that the cavity comes into its steady state after time $t \gg 1/\kappa$. As such, the rate of incoming photons should be larger than the rate of loss, ie $\langle\hat{b}_{1_{\text{in}}}^\dagger\hat{b}_{1_{\text{in}}}\rangle \gg \kappa$, to ensure $\langle\hat{N}_{c_1}\rangle = \langle\hat{c}_1^\dagger\hat{c}_1\rangle \gg 1$. In our numerical simulations we have fixed the total interaction time $\tau = 10^{-4} >> 1/\kappa = 10^{-6}$ and we change the number of cavity photons, which is the parameter affecting the dynamics of our system, by just changing the intensity of the incoming light field $\langle\hat{b}_{1_{\text{in}}}^\dagger\hat{b}_{1_{\text{in}}}\rangle$.

We measure a combined signal of the same form as in the free space case, but now we measure an observable of the output field, $\hat{b}_{1_{\text{out}}}(t)$, since we do not have any direct access to the cavity mode. The output field contains information about atomic observables through Eq. (58). Similarly with Sec. (IV B) we use as our light observable the difference of the phase quadratures of a specific mode of the output fields.

We plot ξ_{s_2} for the same area values as for Fig. [6]-[8] with $\kappa = 10^6$ Hz. Here, we noticed that for $\Delta = 10^2$GHz and area values smaller than $A = 10^{-8}\text{m}^2$ we have to decrease the incoming light intensity at a level that we tend to a regime where $\langle\hat{N}_{c_1}\rangle \to 1$. We can avoid that by

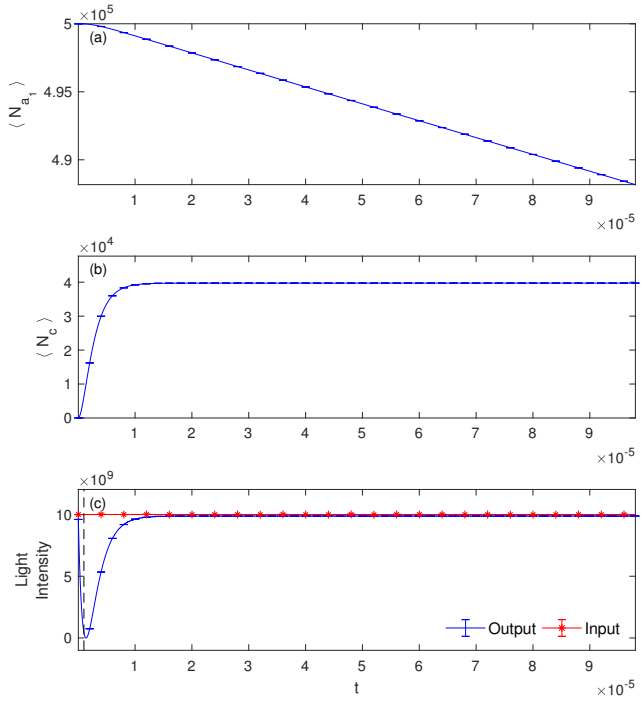

FIG. 14. Cavity dynamics: time evolution of (a) mean number of atoms in state $|1\rangle$, $\langle N_{a_1}\rangle$, (b) mean number of cavity photons $\langle N_{c_1}\rangle$, (c) Intensity of input light (solid line with asterisks) and intensity of the leaking output light field from the cavity (solid line). The vertical dashed line is drawn at the time point $1/\kappa$. We notice that we need $\tau \gg 1/\kappa$, in order to reach the cavity steady state. Other parameter values: $A = 10^{-8}\mathrm{m}^2$, $\Delta = 10^2\,\mathrm{GHz}$, $N_a = 10^6$ and $\kappa = 1\,\mathrm{MHz}$.

just appropriately increasing the detuning $\Delta = 10^4$GHz, in order to obtain the same interaction strength. Assuming a cavity of length $L = 10$ cm, this corresponds to a finesse of $\sim 10^4$. Our choice of cavity parameters is similar to those reported in [81], and is motivated by a cavity that could be added to an existing atom interferometry set-up, and can be installed outside the vacuum system. We use a range of different intensities for the incoming light field to determine the best sensitivity. Comparing Fig. [6]-[8] with Fig. [15] it is apparent that we achieve better sensitivities by adding a cavity, than just using free space light fields. Although we don't have any analytical results for the case of the cavity, due to the complexity of that model, we examined numerically if the dynamics of the system has the same behaviour as in the free space case. We concluded that we can find the optimum of the sensitivity using the same procedure as in Sec. [VI]. Namely for a particular value of A (or equivalently $V = AL$) and N_a we can find the minimum of ξ_{s_2} with respect to the remaining parameters N_{c_1}/Δ_1^2. Here we have one parameter more, the photon decay rate from the cavity, κ. We notice that we have better sensitivities for smaller values of κ, thus for larger cavity quality factors (see Fig. [16]). However, in the cavity case we are more constrained on the parameter values we could use, as they should satisfy $\langle \hat{b}^\dagger_{1_{\rm in}} \hat{b}_{1_{\rm in}}\rangle > \kappa$ and $\tau > 1/\kappa$ as we discussed earlier.

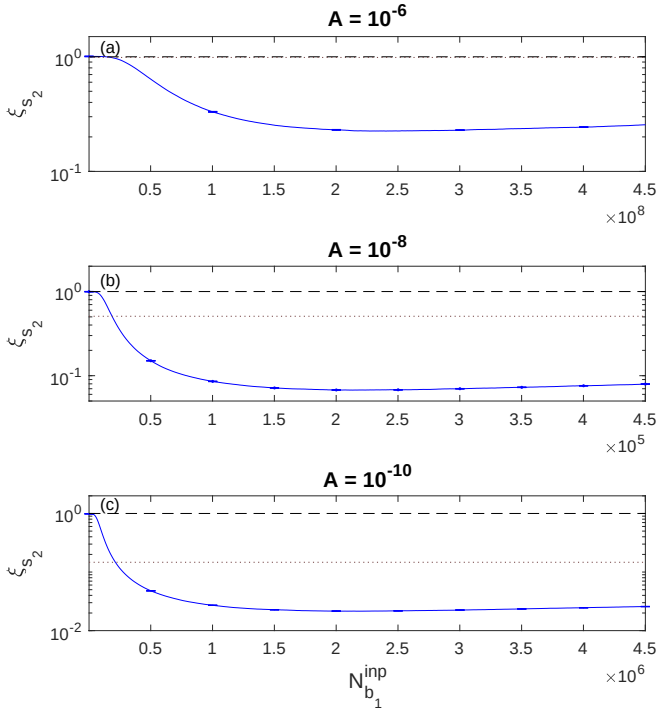

FIG. 15. Cavity: ξ_s with respect to $N_{b_1}^{\rm inp}$ for different values of A. The dotted lines show the $\min(\xi_{s_2})$ of the corresponding cases in Fig. [6] - [8]. The dashed lines represent the SNL. The parameter values are $N_a = 10^6$ and $\kappa = 1\,\mathrm{MHz}$ and $\Delta = 10^2$ GHz, except (c) where we used $\Delta = 10^4$ GHz, for the reasons discussed in the main text.

X. CONCLUSION

We have analysed the creation of spin-squeezing in an ensemble of Bose-condensed atoms via quantum non-demolition measurement, considering both freely propagating light, and optical cavities. We found that the determining factor in the quality of spin-squeezing produced was the cross-sectional area of the optical beam used to probe the spin of the atomic system, with small areas leading to higher atom-light coupling, and a larger phase shift on the light for a given level of spontaneous emission. Of course, varying the intensity, detuning, or duration of the incoming light also affects the level of spin squeezing. However, for a given area, fixing two of these parameters while adjusting the remaining one would always lead to the same optimum. For the D2

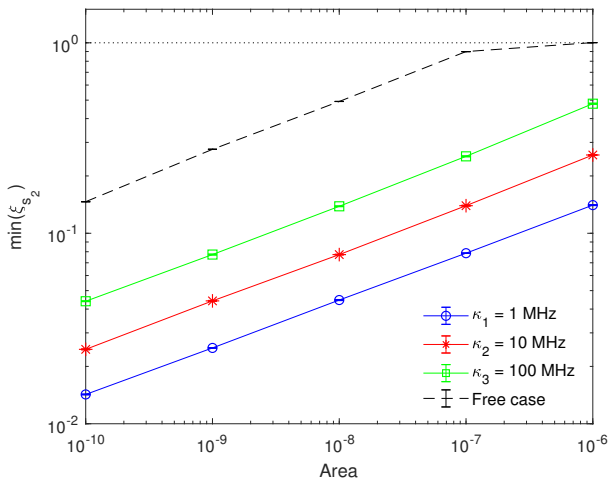

FIG. 16. Minimum value of ξ_{s_2} with respect to the area, for three different values of κ for the cavity case. We also plot the free space case (dashed line). The dotted line represents the SNL. The other parameter values are $N_a = 10^6$ and $\Delta = 10^2$ GHz, except for the area values $A = 10^{-9}\text{m}^2$ and $A = 10^{-10}\text{m}^2$ in all cavity lines where we used $\Delta = 10^4$GHz, for the reasons we mentioned in the main text.

transition in ^{87}Rb atoms, we found that for the case of freely propagating light, no squeezing was possible when the cross-sectional area of the atom-light interaction was larger than $\sim 10^{-6}$ m^2 due to loss of atoms due to spontaneous emission, regardless of the intensity or detuning of the incoming light. For areas less than this, we found significant spin-squeezing was possible, with an area of 10^{-11} m^2 leading to a spin squeezing value of $\sim 3\times10^{-2}$, which corresponds to a potential improvement of atom interferometric sensitivity of ~ 33, which is equivalent to increasing the number of atoms by a factor of 1000. The use of optical squeezing improved the level of quantum enhancement further, and relaxed the restrictions on the area of the light. Finally, we considered the use of an optical cavity. For reasonably achievable cavity parameters, we found approximately an order of magnitude increase over what was achievable in the free space case.

XI. ACKNOWLEDGEMENTS

The authors would like to acknowledge useful discussions with Barry Garraway, Stuart Szigetti, Joseph Hope, and John Close. M.K. and J.A.D. received funding from UK EPSRC through the Networked Quantum Information Technology (NQIT) Hub, Grant No. EP/M013243/1.

[1] Alexander D. Cronin, Jörg Schmiedmayer, and David E. Pritchard, "Optics and interferometry with atoms and molecules," Rev. Mod. Phys. **81**, 1051–1129 (2009).
[2] N. P. Robins, P. A. Altin, J. E. Debs, and J. D. Close, "Atom lasers: Production, properties and prospects for precision inertial measurement," Physics Reports **529**, 265–296 (2013).
[3] Mattias Johnsson, Simon Haine, Joseph Hope, Nick Robins, Cristina Figl, Matthew Jeppesen, Julien Dugué, and John Close, "Semiclassical limits to the linewidth of an atom laser," Phys. Rev. A **75**, 043618 (2007).
[4] J. E. Debs, P. A. Altin, T. H. Barter, D. Döring, G. R. Dennis, G. McDonald, R. P. Anderson, J. D. Close, and N. P. Robins, "Cold-atom gravimetry with a bose-einstein condensate," Phys. Rev. A **84**, 033610 (2011).
[5] S. S. Szigeti, J. E. Debs, J. J. Hope, N. P. Robins, and J. D. Close, "Why momentum width matters for atom interferometry with Bragg pulses," New Journal of Physics **14**, 023009 (2012).
[6] G. D. McDonald, C. C. N. Kuhn, S. Bennetts, J. E. Debs, K. S. Hardman, M. Johnsson, J. D. Close, and N. P. Robins, "80$\hbar k$ momentum separation with bloch oscillations in an optically guided atom interferometer," Phys. Rev. A **88**, 053620 (2013).
[7] Michail Kritsotakis, Stuart S. Szigeti, Jacob A. Dunningham, and Simon A. Haine, "Optimal matter-wave gravimetry," Phys. Rev. A **98**, 023629 (2018).
[8] D. J. Wineland, J. J. Bollinger, W. M. Itano, F. L. Moore, and D. J. Heinzen, "Spin squeezing and reduced quantum noise in spectroscopy," Phys. Rev. A **46**, R6797–R6800 (1992).
[9] Masahiro Kitagawa and Masahito Ueda, "Squeezed spin states," Phys. Rev. A **47**, 5138–5143 (1993).
[10] Anders S. Sørensen and Klaus Mølmer, "Entanglement and extreme spin squeezing," Phys. Rev. Lett. **86**, 4431–4434 (2001).
[11] Luca Pezzè, Augusto Smerzi, Markus K. Oberthaler, Roman Schmied, and Philipp Treutlein, "Quantum metrology with nonclassical states of atomic ensembles," Rev. Mod. Phys. **90**, 035005 (2018).
[12] L.-M. Duan, A. Sørensen, J. I. Cirac, and P. Zoller, "Squeezing and entanglement of atomic beams," Phys. Rev. Lett. **85**, 3991–3994 (2000).
[13] H. Pu and P. Meystre, "Creating macroscopic atomic Einstein-Podolsky-Rosen states from Bose-Einstein condensates," Phys. Rev. Lett. **85**, 3987–3990 (2000).
[14] Anders Søndberg Sørensen, "Bogoliubov theory of entanglement in a Bose-Einstein condensate," Phys. Rev. A **65**, 043610 (2002).
[15] A. Micheli, D. Jaksch, J. I. Cirac, and P. Zoller, "Many-particle entanglement in two-component Bose-Einstein condensates," Phys. Rev. A **67**, 013607 (2003).
[16] K. V. Kheruntsyan, M. K. Olsen, and P. D. Drummond, "Einstein-Podolsky-Rosen correlations via dissociation of a molecular Bose-Einstein condensate," Phys. Rev. Lett. **95**, 150405 (2005).
[17] Mattias T. Johnsson and Simon A. Haine, "Generating quadrature squeezing in an atom laser through self-interaction," Phys. Rev. Lett. **99**, 010401 (2007).

[18] Yun Li, P. Treutlein, J. Reichel, and A. Sinatra, "Spin squeezing in a bimodal condensate: spatial dynamics and particle losses," The European Physical Journal B **68**, 365–381 (2009).

[19] Safoura S. Mirkhalaf, Samuel P. Nolan, and Simon A. Haine, "Robustifying twist-and-turn entanglement with interaction-based readout," Phys. Rev. A **97**, 053618 (2018).

[20] A. Kuzmich, Klaus Mølmer, and E. Polzik, "Spin squeezing in an ensemble of atoms illuminated with squeezed light," Phys. Rev. Lett. **79**, 4782–4785 (1997).

[21] Kuzmich, A., Bigelow, N. P., and Mandel, L., "Atomic quantum non-demolition measurements and squeezing," Europhys. Lett. **42**, 481–486 (1998).

[22] M. G. Moore, O. Zobay, and P. Meystre, "Quantum optics of a Bose-Einstein condensate coupled to a quantized light field," Phys. Rev. A **60**, 1491–1506 (1999).

[23] A. Kuzmich, L. Mandel, and N. P. Bigelow, "Generation of spin squeezing via continuous quantum nondemolition measurement," Phys. Rev. Lett. **85**, 1594–1597 (2000).

[24] Hui Jing, Jing-Ling Chen, and Mo-Lin Ge, "Quantum-dynamical theory for squeezing the output of a Bose-Einstein condensate," Phys. Rev. A **63**, 015601 (2000).

[25] Michael Fleischhauer and Shangqing Gong, "Stationary source of nonclassical or entangled atoms," Phys. Rev. Lett. **88**, 070404 (2002).

[26] S. A. Haine and J. J. Hope, "Outcoupling from a Bose-Einstein condensate with squeezed light to produce entangled-atom laser beams," Phys. Rev. A **72**, 033601 (2005).

[27] S. A. Haine and J. J. Hope, "A multi-mode model of a non-classical atom laser produced by outcoupling from a Bose-Einstein condensate with squeezed light," Laser Physics Letters **2**, 597–602 (2005).

[28] S R de Echaniz, M W Mitchell, M Kubasik, M Koschorreck, H Crepaz, J Eschner, and E S Polzik, "Conditions for spin squeezing in a cold ^{87}Rb ensemble," Journal of Optics B: Quantum and Semiclassical Optics **7**, S548–S552 (2005).

[29] S. A. Haine, M. K. Olsen, and J. J. Hope, "Generating controllable atom-light entanglement with a Raman atom laser system," Phys. Rev. Lett. **96**, 133601 (2006).

[30] Klemens Hammerer, Anders S. Sørensen, and Eugene S. Polzik, "Quantum interface between light and atomic ensembles," Rev. Mod. Phys. **82**, 1041–1093 (2010).

[31] S. A. Haine, "Information-recycling beam splitters for quantum enhanced atom interferometry," Phys. Rev. Lett. **110**, 053002 (2013).

[32] Graciana Puentes, Giorgio Colangelo, Robert J Sewell, and Morgan W Mitchell, "Planar squeezing by quantum non-demolition measurement in cold atomic ensembles," New Journal of Physics **15**, 103031 (2013).

[33] Stuart S. Szigeti, Behnam Tonekaboni, Wing Yung S. Lau, Samantha N. Hood, and Simon A. Haine, "Squeezed-light-enhanced atom interferometry below the standard quantum limit," Phys. Rev. A **90**, 063630 (2014).

[34] Behnam Tonekaboni, Simon A. Haine, and Stuart S. Szigeti, "Heisenberg-limited metrology with a squeezed vacuum state, three-mode mixing, and information recycling," Phys. Rev. A **91**, 033616 (2015).

[35] Simon A. Haine, Stuart S. Szigeti, Matthias D. Lang, and Carlton M. Caves, "Heisenberg-limited metrology with information recycling," Phys. Rev. A **91**, 041802 (2015).

[36] Simon A. Haine and Stuart S. Szigeti, "Quantum metrology with mixed states: When recovering lost information is better than never losing it," Phys. Rev. A **92**, 032317 (2015).

[37] Simon A. Haine and Wing Yung Sarah Lau, "Generation of atom-light entanglement in an optical cavity for quantum enhanced atom interferometry," Phys. Rev. A **93**, 023607 (2016).

[38] Leonardo Salvi, Nicola Poli, Vladan Vuletić, and Guglielmo M. Tino, "Squeezing on momentum states for atom interferometry," Phys. Rev. Lett. **120**, 033601 (2018).

[39] J. Esteve, C. Gross, A. Weller, S. Giovanazzi, and M. K. Oberthaler, "Squeezing and entanglement in a Bose-Einstein condensate," Nature **455**, 1216 (2008).

[40] C. Gross, T. Zibold, E. Nicklas, J. Esteve, and M. K. Oberthaler, "Nonlinear atom interferometer surpasses classical precision limit," Nature **464**, 1165–1169 (2010).

[41] Max F. Riedel, Pascal Böhi, Yun Li, Theodor W. Hänsch, Alice Sinatra, and Philipp Treutlein, "Atom-chip-based generation of entanglement for quantum metrology," Nature **464**, 1170–1173 (2010).

[42] B. Lücke, M. Scherer, J. Kruse, L. Pezze, F. Deuretzbacher, P. Hyllus, O. Topic, J. Peise, W. Ertmer, J. Arlt, L. Santos, A. Smerzi, and C. Klempt, "Twin matter waves for interferometry beyond the classical limit," Science **334**, 773–776 (2011).

[43] C. D. Hamley, C. S. Gerving, T. M. Hoang, E. M. Bookjans, and M. S. Chapman, "Spin-nematic squeezed vacuum in a quantum gas," Nat Phys **8**, 305–308 (2012).

[44] Helmut Strobel, Wolfgang Muessel, Daniel Linnemann, Tilman Zibold, David B. Hume, Luca Pezzè, Augusto Smerzi, and Markus K. Oberthaler, "Fisher information and entanglement of non-Gaussian spin states," Science **345**, 424–427 (2014).

[45] W. Muessel, H. Strobel, D. Linnemann, D. B. Hume, and M. K. Oberthaler, "Scalable spin squeezing for quantum-enhanced magnetometry with Bose-Einstein condensates," Phys. Rev. Lett. **113**, 103004 (2014).

[46] I. Kruse, K. Lange, J. Peise, B. Lücke, L. Pezzè, J. Arlt, W. Ertmer, C. Lisdat, L. Santos, A. Smerzi, and C. Klempt, "Improvement of an atomic clock using squeezed vacuum," Phys. Rev. Lett. **117**, 143004 (2016).

[47] D. Linnemann, H. Strobel, W. Muessel, J. Schulz, R. J. Lewis-Swan, K. V. Kheruntsyan, and M. K. Oberthaler, "Quantum-enhanced sensing based on time reversal of nonlinear dynamics," Phys. Rev. Lett. **117**, 013001 (2016).

[48] Yi-Quan Zou, Ling-Na Wu, Qi Liu, Xin-Yu Luo, Shuai-Feng Guo, Jia-Hao Cao, Meng Khoon Tey, and Li You, "Beating the classical precision limit with spin-1 Dicke states of more than 10,000 atoms," Proceedings of the National Academy of Sciences **115**, 6381–6385 (2018), https://www.pnas.org/content/115/25/6381.full.pdf.

[49] Simon A. Haine and Mattias T. Johnsson, "Dynamic scheme for generating number squeezing in Bose-Einstein condensates through nonlinear interactions," Phys. Rev. A **80**, 023611 (2009).

[50] S. A. Haine and A. J. Ferris, "Surpassing the standard quantum limit in an atom interferometer with four-mode entanglement produced from four-wave mixing," Phys. Rev. A **84**, 043624 (2011).

[51] B. Opanchuk, M. Egorov, S. Hoffmann, A. I. Sidorov, and P. D. Drummond, "Quantum noise in three-dimensional BEC interferometry," EPL (Europhysics Letters) **97**, 50003 (2012).

[52] S. A. Haine, J. Lau, R. P. Anderson, and M. T. Johnsson, "Self-induced spatial dynamics to enhance spin squeezing via one-axis twisting in a two-component Bose-Einstein condensate," Phys. Rev. A **90**, 023613 (2014).

[53] Samuel P. Nolan, Jacopo Sabbatini, Michael W. J. Bromley, Matthew J. Davis, and Simon A. Haine, "Quantum enhanced measurement of rotations with a spin-1 Bose-Einstein condensate in a ring trap," Phys. Rev. A **93**, 023616 (2016).

[54] Simon A Haine, "Quantum noise in bright soliton matter-wave interferometry," New Journal of Physics **20**, 033009 (2018).

[55] J. Appel, P. J. Windpassinger, D. Oblak, U. B. Hoff, N. Kjaergaard, and E. S. Polzik, "Mesoscopic atomic entanglement for precision measurements beyond the standard quantum limit," Proceedings of the National Academy of Sciences **106**, 10960–10965 (2009).

[56] Anne Louchet-Chauvet, Jürgen Appel, Jelmer J Renema, Daniel Oblak, Niels Kjaergaard, and Eugene S Polzik, "Entanglement-assisted atomic clock beyond the projection noise limit," New Journal of Physics **12**, 065032 (2010).

[57] Monika H. Schleier-Smith, Ian D. Leroux, and Vladan Vuletić, "Squeezing the collective spin of a dilute atomic ensemble by cavity feedback," Phys. Rev. A **81**, 021804 (2010).

[58] Monika H. Schleier-Smith, Ian D. Leroux, and Vladan Vuletić, "States of an ensemble of two-level atoms with reduced quantum uncertainty," Phys. Rev. Lett. **104**, 073604 (2010).

[59] Ian D. Leroux, Monika H. Schleier-Smith, and Vladan Vuletić, "Implementation of cavity squeezing of a collective atomic spin," Phys. Rev. Lett. **104**, 073602 (2010).

[60] M. Koschorreck, M. Napolitano, B. Dubost, and M. W. Mitchell, "Quantum nondemolition measurement of large-spin ensembles by dynamical decoupling," Phys. Rev. Lett. **105**, 093602 (2010).

[61] R. J. Sewell, M. Koschorreck, M. Napolitano, B. Dubost, N. Behbood, and M. W. Mitchell, "Magnetic sensitivity beyond the projection noise limit by spin squeezing," Phys. Rev. Lett. **109**, 253605 (2012).

[62] R. J. Sewell, M. Napolitano, N. Behbood, G. Colangelo, F. Martin Ciurana, and M. W. Mitchell, "Ultrasensitive atomic spin measurements with a nonlinear interferometer," Phys. Rev. X **4**, 021045 (2014).

[63] Onur Hosten, Nils J. Engelsen, Rajiv Krishnakumar, and Mark A. Kasevich, "Measurement noise 100 times lower than the quantum-projection limit using entangled atoms," Nature **529**, 505 EP – (2016).

[64] P A Altin, M T Johnsson, V Negnevitsky, G R Dennis, R P Anderson, J E Debs, S S Szigeti, K S Hardman, S Bennetts, G D McDonald, L D Turner, J D Close, and N P Robins, "Precision atomic gravimeter based on Bragg diffraction," New Journal of Physics **15**, 023009 (2013).

[65] M. Kasevich and S. Chu, "Measurement of the gravitational acceleration of an atom with a light-pulse atom interferometer," Applied Physics B: Lasers and Optics **54**, 321–332 (1992), 10.1007/BF00325375.

[66] F. Riehle, Th. Kisters, A. Witte, J. Helmcke, and Ch. J. Bordé, "Optical Ramsey spectroscopy in a rotating frame: Sagnac effect in a matter-wave interferometer," Phys. Rev. Lett. **67**, 177–180 (1991).

[67] Wolfgang P. Schleich, Daniel M. Greenberger, and Ernst M. Rasel, "Redshift controversy in atom interferometry: Representation dependence of the origin of phase shift," Phys. Rev. Lett. **110**, 010401 (2013).

[68] Stephan Kleinert, Endre Kajari, Albert Roura, and Wolfgang P. Schleich, "Representation-free description of light-pulse atom interferometry including non-inertial effects," Physics Reports **605**, 1 – 50 (2015).

[69] A. Bertoldi, F. Minardi, and M. Prevedelli, "Phase shift in atom interferometers: Corrections for nonquadratic potentials and finite-duration laser pulses," Phys. Rev. A **99**, 033619 (2019).

[70] J. M. Radcliffe, "Some properties of coherent spin states," Journal of Physics A: General Physics **4**, 313 (1971).

[71] Stuart S. Szigeti, Samuel P. Nolan, John D. Close, and Simon A. Haine, "High-precision quantum-enhanced gravimetry with a bose-einstein condensate," Phys. Rev. Lett. **125**, 100402 (2020).

[72] CW Gardiner and MJ Collett, "Input and output in damped quantum systems: Quantum stochastic differential equations and the master equation," Physical Review A **31**, 3761 (1985).

[73] Etienne Brion, Line Hjortshøj Pedersen, and Klaus Mølmer, "Adiabatic elimination in a lambda system," Journal of Physics A: Mathematical and Theoretical **40**, 1033 (2007).

[74] Hans A. Bachor and Timothy C. Ralph, *A Guide to Experiments in Quantum Optics*, 2nd ed. (Wiley, 2004).

[75] Lu-Ming Duan, J. I. Cirac, P. Zoller, and E. S. Polzik, "Quantum communication between atomic ensembles using coherent light," Phys. Rev. Lett. **85**, 5643–5646 (2000).

[76] Lars Bojer Madsen and Klaus Mølmer, "Spin squeezing and precision probing with light and samples of atoms in the Gaussian description," Physical Review A **70**, 052324 (2004).

[77] Crispin Gardiner and Peter Zoller, *Quantum noise: a handbook of Markovian and non-Markovian quantum stochastic methods with applications to quantum optics*, Vol. 56 (Springer Science & Business Media, 2004).

[78] D. A. Steck, "Rubidium 87 d line data," revision 2.1.5, 13 January (2015).

[79] KM Mertes, JW Merrill, R Carretero-González, DJ Frantzeskakis, PG Kevrekidis, and DS Hall, "Nonequilibrium dynamics and superfluid ring excitations in binary Bose-Einstein condensates," Physical Review Letters **99**, 190402 (2007).

[80] D. F. Walls and G. J. Milburn, *Quantum Optics*, 2nd ed. (Springer-Verlag, Berlin and Heidelberg, 2008).

[81] R. Poldy, B. C. Buchler, P. A. Altin, N. P. Robins, and J. D. Close, "Feasibility of squeezing measurements with cavity-based atom detection," Phys. Rev. A **86**, 043806 (2012).

Appendix A: Introduction

We consider the combined signal

$$\hat{S}_2(\tau) = \hat{J}_z(\tau) - \hat{J}_z^{\rm inf}(\tau), \tag{A1}$$

where

$$\hat{J}_z^{\rm inf}(\tau) = G\hat{S}_b(\tau) \qquad \hat{S}_b(\tau) = \hat{Y}_2(\tau) - \hat{Y}_1(\tau). \tag{A2}$$

For simplicity in the following we will present the time dependence explicitly only in our final results or when it is considered necessary. The variance of $\hat{S}_2$ would be given by

$$\mathrm{Var}(\hat{S}_2) = \mathrm{Var}(\hat{J}_z) + G^2\mathrm{Var}(\hat{S}_b) - 2G\mathrm{Cov}(\hat{J}_z, \hat{S}_b), \tag{A3}$$

since $\mathrm{Cov}(\hat{J}_z, \hat{S}_b) = \mathrm{Cov}(\hat{S}_b, \hat{J}_z)$. We minimise $\mathrm{Var}(\hat{S}_2)$ with respect to G

$$G = \frac{\mathrm{Cov}(\hat{J}_z, \hat{S}_b)}{\mathrm{Var}(\hat{S}_b)}. \tag{A4}$$

Inserting that back in Eq. (A3) we get

$$\mathrm{Var}(\hat{S}_2) = \mathrm{Var}(\hat{J}_z) - \frac{\mathrm{Cov}^2(\hat{J}_z, \hat{S}_b)}{\mathrm{Var}(\hat{S}_b)}. \tag{A5}$$

So, in order to calculate $\mathrm{Var}(\hat{S}_2)$ we need the covariance between $\hat{J}_z$ and $\hat{S}_b$, $\mathrm{Cov}(\hat{J}_z, \hat{S}_b)$, and the variance of the phase quadrature of the light field $\mathrm{Var}(\hat{Y}_1)$, since $\mathrm{Var}(\hat{Y}_1) = \mathrm{Var}(\hat{Y}_2)$ and $\mathrm{Cov}(\hat{Y}_2, \hat{Y}_1) = 0$, thus $\mathrm{Var}(\hat{S}_b) = 2\mathrm{Var}(\hat{Y}_1)$. At the end we calculate the squeezing parameter, which in our case ($\theta = 0$) is given by

$$\xi_{s_2} = \sqrt{N_a}\frac{\sqrt{\mathrm{Var}(\hat{S}_2)}}{\langle \hat{J}_x \rangle}. \tag{A6}$$

Appendix B: No Spontaneous Emission

1. Atomic Expectation Values

The atomic equations with no spontaneous emission are given by

$$\hat{a}_1(t) = \hat{a}_1(0)e^{i\frac{g^2}{\Delta}\int_0^t \hat{b}_{01}^\dagger(t')\hat{b}_{01}(t')dt'} \tag{B1}$$

$$\hat{a}_1^\dagger(t) = \hat{a}_1^\dagger(0)e^{-i\frac{g^2}{\Delta}\int_0^t \hat{b}_{01}^\dagger(t')\hat{b}_{01}(t')dt'}. \tag{B2}$$

Hence, the atomic population operator is independent of time

$$\hat{N}_{a_1}(t) = \hat{a}_1^\dagger(t)\hat{a}_1(t) = \hat{a}_1^\dagger(0)\hat{a}_1(0). \tag{B3}$$

We consider that our total state initially is given by the product

$$|\Psi\rangle = |\alpha_1\rangle \otimes |\alpha_2\rangle \otimes |\beta_1\rangle \otimes |\beta_2\rangle \otimes |0\rangle, \tag{B4}$$

meaning that the atomic ensemble, as well as the two light fields are in coherent states while the bath is described by the vacuum state, giving the following expectation values

$$\hat{a}_1(0)|\alpha_1\rangle = \sqrt{\frac{N_a}{2}}|\alpha_1\rangle, \qquad \hat{b}_{01}(t)|\beta_1\rangle = \beta_0|\beta_1\rangle, \qquad \hat{q}_{1_{\rm in}}(t)|0\rangle = 0|0\rangle$$

$$\hat{a}_2(0)|\alpha_2\rangle = \sqrt{\frac{N_a}{2}}|\alpha_2\rangle \qquad \hat{b}_{02}(t)|\beta_2\rangle = \beta_0|\beta_2\rangle \qquad \hat{q}_{2_{in}}(t)|0\rangle = 0|0\rangle, \tag{B5}$$

where we have used again $\hat{b}_{0j}(t) = \hat{b}_j(z_L, t)$ with $j = 1, 2$ for simplicity, and we have considered that $\alpha_1(0) = \alpha_2(0) = \sqrt{N_a/2}$ and $\hat{b}_{01}(t) = \hat{b}_{02}(t) = \beta_0$. Now it is really simple to calculate the atomic expectation values in that case

$$\langle \hat{N}_{a_1}(t)\rangle = \frac{N_a}{2}, \qquad \langle \hat{N}_{a_1}^2(t)\rangle = \langle \hat{N}_{a_1}^2(t')\rangle = \langle \hat{N}_{a_1}^2(0)\rangle = \frac{N_a}{2} + \frac{N_a^2}{4}. \tag{B6}$$

2. Phase Quadrature

The light equation in the case of no spontaneous emission is

$$\hat{b}_1(z_R,t) = \hat{b}_{01}(t)e^{i\frac{g^2}{c\Delta}\hat{a}_1^\dagger(t)\hat{a}_1(t)}, \tag{B7}$$

We select a specific mode of the light field

$$\hat{\mathcal{b}}_1(\tau) = \frac{\sqrt{c}}{\sqrt{\tau}}\int_0^\tau \hat{b}_1(z_R,t)dt. \tag{B8}$$

Here the atomic population is constant, thus

$$\hat{\mathcal{b}}_1(\tau) = \frac{\sqrt{c}}{\sqrt{\tau}}e^{i\frac{g^2}{c\Delta}\hat{a}_1^\dagger(t)\hat{a}_1(t)}\int_0^\tau \hat{b}_{01}(t)dt. \tag{B9}$$

We know that the incident light field obeys the following commutation relation $[\hat{b}_{01}(t),\hat{b}_{01}^\dagger(t')] = \frac{1}{c}\delta(t-t')$. We find the phase quadrature of the specific mode

$$\hat{Y}_1(\tau) \equiv i(\hat{\mathcal{b}}_1(\tau) - \hat{\mathcal{b}}_1^\dagger(\tau)) = i\frac{\sqrt{c}}{\sqrt{\tau}}\left(e^{i\frac{g^2}{c\Delta}\hat{a}_1^\dagger(t)\hat{a}_1(t)}\int_0^\tau \hat{b}_{01}(t)dt - e^{-i\frac{g^2}{c\Delta}\hat{a}_1^\dagger(t)\hat{a}_1(t)}\int_0^\tau \hat{b}_{01}^\dagger(t)dt\right). \tag{B10}$$

We make the small angle approximation

$$\frac{g^2}{c\Delta}\hat{a}_1^\dagger(t)\hat{a}_1(t) << 1, \tag{B11}$$

and we get

$$\hat{Y}_1(\tau) \approx \hat{Y}_{1_{\rm in}}(\tau) - \frac{g^2}{\sqrt{c\tau}\Delta}\hat{a}_1^\dagger(\tau)\hat{a}_1(\tau)\int_0^\tau \left(\hat{b}_{01}(t)+\hat{b}_{01}^\dagger(t)\right)dt, \tag{B12}$$

where

$$\hat{Y}_{1_{\rm in}}(\tau) = i\frac{\sqrt{c}}{\sqrt{\tau}}\int_0^\tau \left(\hat{b}_{01}(t)-\hat{b}_{01}^\dagger(t)\right)dt. \tag{B13}$$

We calculate the expectation value of the phase quadrature

$$\langle\hat{Y}_1(\tau)\rangle \approx -\frac{g^2N_a\beta_0\tau}{\Delta\sqrt{c\tau}}, \tag{B14}$$

where we have used that $\langle\hat{Y}_{1_{\rm in}}(\tau)\rangle = 0$ and assumed that $\beta_0 = \beta_0^*$. We calculate the square of the phase quadrature

$$\hat{Y_1}^2(\tau) \approx \hat{Y}_{1_{\rm in}}^2(\tau) + \frac{g^4}{c\tau\Delta^2}\hat{a}_1^\dagger(\tau)\hat{a}_1(\tau)\hat{a}_1^\dagger(\tau)\hat{a}_1(\tau)\int_0^\tau\int_0^\tau dtdt'\ \left(\hat{b}_{01}(t)+\hat{b}_{01}^\dagger(t)\right)\left(\hat{b}_{01}(t')+\hat{b}_{01}^\dagger(t')\right). \tag{B15}$$

For simplicity we calculate separately

$$Q_1 = \int_0^\tau\int_0^\tau dtdt'\ \left(\hat{b}_{01}(t)\hat{b}_{01}(t') + \hat{b}_{01}(t)\hat{b}_{01}^\dagger(t') + \hat{b}_{01}^\dagger(t)\hat{b}_{01}(t') + \hat{b}_{01}^\dagger(t)\hat{b}_{01}^\dagger(t')\right). \tag{B16}$$

After using the commutation relation $\left[\hat{b}_{01}(t),\hat{b}_{01}^\dagger(t')\right] = \frac{1}{c}\delta(t-t')$ and the delta function property $\int_0^\tau \delta(t-t')dt' = 1$ we obtain

$$\langle Q_1\rangle = 4\beta_0^2\tau^2 + \frac{\tau}{c}. \tag{B17}$$

Making use of the same commutation relation and the same property of the delta function we find that $\langle\hat{Y}_{1_{\rm in}}^2(\tau)\rangle = 1$. Thus,

$$\langle\hat{Y}_1^2(\tau)\rangle \approx 1 + \frac{g^4}{c\tau\Delta^2}\left(\frac{N_a}{2}+\frac{N_a^2}{4}\right)\left(4\beta_0^2\tau^2+\frac{\tau}{2c}\right), \tag{B18}$$

where we have used Eq. (B6). For simplicity, we can ignore the last term of Eq. (B18) since $4\beta_0^2\tau^2 >> \tau/2c$

$$\langle \hat{Y}_1^2(\tau)\rangle \approx 1 + \frac{4g^4\beta_0^2\tau^2}{c\tau\Delta^2}\left(\frac{N_a}{2} + \frac{N_a^2}{4}\right). \tag{B19}$$

From Eq. (B14) we have

$$\langle \hat{Y}_1(\tau)\rangle^2 \approx \frac{g^4\beta_0^2 N_a^2\tau^2}{c\tau\Delta^2}. \tag{B20}$$

Hence, we finally have

$$\mathrm{Var}(\hat{Y}_1(\tau)) \approx 1 + 2\chi_{\mathrm{ns}}^2 N_a N_{\mathrm{ph}}, \tag{B21}$$

and

$$\mathrm{Var}(\hat{S}_b) = 2\mathrm{Var}(\hat{Y}_1(\tau)) \approx 2 + 4\chi_{\mathrm{ns}}^2 N_a N_{\mathrm{ph}}, \tag{B22}$$

where we have defined

$$\chi_{\mathrm{ns}} \equiv \frac{g^2}{c\Delta} \qquad N_{\mathrm{ph}} \equiv \beta_0^2\tau. \tag{B23}$$

3. Covariances

The covariance of $\hat{J}_z(\tau)$ and $\hat{S}_b(\tau)$ is defined as

$$\mathrm{Cov}(\hat{J}_z(\tau), \hat{S}_b(\tau)) = \langle \hat{J}_z(\tau)\hat{S}_b(\tau)\rangle - \langle \hat{J}_z(\tau)\rangle\langle \hat{S}_b(\tau)\rangle. \tag{B24}$$

We know that $\langle \hat{S}_b(\tau)\rangle = 0$, since $\hat{S}_b = \hat{Y}_2 - \hat{Y}_1$. Hence,

$$\mathrm{Cov}(\hat{J}_z(\tau), \hat{S}_b(\tau)) = \langle \hat{J}_z(\tau)\hat{Y}_2(\tau)\rangle - \langle \hat{J}_z(\tau)\hat{Y}_1(\tau)\rangle. \tag{B25}$$

Using $\hat{J}_z(\tau) = (\hat{N}_{a_1}(\tau) - \hat{N}_{a_2}(\tau))/2$, Eq. (B12) and the atomic expectation values from Sec. (B 1) we obtain

$$\mathrm{Cov}(\hat{J}_z(\tau), \hat{S}_b(\tau)) \approx \chi_{\mathrm{ns}} N_a \sqrt{N_{\mathrm{ph}}}. \tag{B26}$$

4. Quantum Enhancement Parameter ξ_s

Inserting Eq. (B26) and (B22) in (A5) we obtain

$$\mathrm{Var}(\hat{S}_2(\tau)) \approx \frac{N_a}{4}\left(1 - \frac{\chi_{\mathrm{ns}}^2 N_{\mathrm{ph}} N_a}{\chi_{\mathrm{ns}}^2 N_{\mathrm{ph}} N_a + 1/2}\right). \tag{B27}$$

Using the atomic equations of motion we find for small exponents $\chi_{\mathrm{ns}}^2 N_{\mathrm{ph}} << 1$

$$\langle \hat{J}_x(\tau)\rangle \approx \frac{N_a}{2} e^{-\chi_{\mathrm{ns}}^2 N_{\mathrm{ph}}}. \tag{B28}$$

Finally, from Eq. (A6) we obtain

$$\xi_{s_2}^{ns}(\tau) \approx e^{\chi_{\mathrm{ns}}^2 N_{\mathrm{ph}}}\left(1 - \frac{\chi_{\mathrm{ns}}^2 N_{\mathrm{ph}} N_a}{\chi_{\mathrm{ns}}^2 N_{\mathrm{ph}} N_a + 1/2}\right)^{1/2}. \tag{B29}$$

Appendix C: Spontaneous Emission

1. Atomic Expectation Values

In the case where we have incorporated spontaneous emission the calculation of the atomic expectation values is more complicated, since we use the following atomic equations

$$\hat{a}_1(t) = \hat{a}_1(0)e^{ig^2(\Omega+i\Gamma)\int_0^t \hat{b}_{01}^\dagger(t')\hat{b}_{01}(t')dt'} + \\ + \frac{g\sqrt{\gamma_3}}{\Delta - i\gamma_3/2} e^{ig^2(\Omega+i\Gamma)\int_0^t \hat{b}_{01}^\dagger(t')\hat{b}_{01}(t')dt'} \int_0^t dt' \hat{b}_{01}^\dagger(t')\hat{q}_{1_{\rm in}}(t') e^{-ig^2(\Omega+i\Gamma)\int_0^{t'} \hat{b}_{01}^\dagger(t'')\hat{b}_{01}(t'')dt''} \tag{C1a}$$

$$\hat{a}_1^\dagger(t) = \hat{a}_1^\dagger(0)e^{-ig^2(\Omega-i\Gamma)\int_0^t \hat{b}_{01}^\dagger(t')\hat{b}_{01}(t')dt'} + \\ + \frac{g\sqrt{\gamma_3}}{\Delta + i\gamma_3/2} e^{-ig^2(\Omega-i\Gamma)\int_0^t \hat{b}_{01}^\dagger(t')\hat{b}_{01}(t')dt'} \int_0^t dt' \hat{b}_{01}(t')\hat{q}_{1_{\rm in}}^\dagger(t') e^{ig^2(\Omega-i\Gamma)\int_0^{t'} \hat{b}_{01}^\dagger(t'')\hat{b}_{01}(t'')dt''}. \tag{C1b}$$

For simplicity we assume that the intensity operator in the exponentials does not depend on time, namely is a constant number $\hat{b}_{01}^\dagger(t)\hat{b}_{01}(t) \approx \beta_0^2$. We essentially assume here that the atomic loss is due to the average field intensity. We also ignore the unitary part of the exponentials, since they would cancel out during the calculation of the atomic expectation values. So, we finally have

$$\hat{a}_1(t) = \underbrace{\sqrt{\epsilon(t)}\hat{a}_1(0)}_{\hat{A}_1(t)} + \underbrace{\frac{g\sqrt{\gamma_3}}{\Delta - i\gamma_3/2}\sqrt{\epsilon(t)}\int_0^t \sqrt{\epsilon^{-1}(t')}\hat{b}_{01}^\dagger(t')\hat{q}_{1_{\rm in}}(t')dt'}_{\hat{A}_2(t)} \tag{C2}$$

$$\hat{a}_1^\dagger(t) = \underbrace{\sqrt{\epsilon(t)}\hat{a}_1^\dagger(0)}_{\hat{A}_1^\dagger(t)} + \underbrace{\frac{g\sqrt{\gamma_3}}{\Delta + i\gamma_3/2}\sqrt{\epsilon(t)}\int_0^t \sqrt{\epsilon^{-1}(t')}\hat{b}_{01}(t')\hat{q}_{1_{\rm in}}^\dagger(t')dt'}_{\hat{A}_2^\dagger(t)}, \tag{C3}$$

where we have defined

$$\epsilon(t) \equiv e^{-2g^2\Gamma\beta_0^2 t}. \tag{C4}$$

We calculate the expectation value of atoms in state $|1\rangle$

$$\langle \hat{N}_{a_1}(t)\rangle = \langle \hat{a}_1^\dagger(t)\hat{a}_1(t)\rangle = \frac{N_a}{2}\epsilon(t), \tag{C5}$$

where $\epsilon(t)$ indicates the atomic rate of loss in our system at time t. Now we are going to calculate the more complicated expectation value $\langle \hat{N}_{a_1}(t)\hat{N}_{a_1}(t')\rangle$. We have named each term of Eq. (C2) and (C3) for simplicity, in order to clearly show which terms finally survive

$$\langle \hat{N}_{a_1}(t)\hat{N}_{a_1}(t')\rangle = \langle \hat{A}_1^\dagger(t)\hat{A}_1(t)\hat{A}_1^\dagger(t')\hat{A}_1(t')\rangle + \langle \hat{A}_1^\dagger(t)\hat{A}_2(t)\hat{A}_2^\dagger(t')\hat{A}_1(t')\rangle, \tag{C6}$$

where all the other terms in this product are zero since $\langle \hat{q}_{1_{\rm in}}\rangle = \langle \hat{q}_{1_{\rm in}}^\dagger\rangle = \langle \hat{q}_{1_{\rm in}}^\dagger \hat{q}_{1_{\rm in}}\rangle = 0$. The first term of the above equation is easily calculated

$$\langle \hat{A}_1^\dagger(t)\hat{A}_1(t)\hat{A}_1^\dagger(t')\hat{A}_1(t')\rangle = \left(\frac{N_a}{2} + \frac{N_a^2}{4}\right)\epsilon(t)\epsilon(t'). \tag{C7}$$

However the second term is more complicated

$$\langle \hat{A}_1^\dagger(t)\hat{A}_2(t)\hat{A}_2^\dagger(t')\hat{A}_1(t')\rangle = 2g^2\Gamma\epsilon(t)\epsilon(t')\langle \hat{a}_1^\dagger(0)\hat{a}_1(0)\rangle \times \\ \times \int_0^t \int_0^{t'} d\xi ds \sqrt{\epsilon^{-1}(s)}\sqrt{\epsilon^{-1}(\xi)}\langle \hat{b}_{01}^\dagger(s)\hat{b}_{01}(\xi)\rangle \langle \hat{q}_{1_{\rm in}}(s)\hat{q}_{1_{\rm in}}^\dagger(\xi)\rangle. \tag{C8}$$

We use the commutation relation for the temporal part of the Langevin noise

$$\left[\hat{q}_{1_{\rm in}}(s), \hat{q}^{\dagger}_{1_{\rm in}}(\xi)\right] = \delta(\xi - s). \tag{C9}$$

We also make use of the following property of the delta function

$$\int_0^{t'} d\xi f(\xi)\delta(\xi - s) = f(s)\Theta(t' - s), \tag{C10}$$

where $\Theta(t' - s)$ is the Heaviside step function and using $\langle \hat{b}^{\dagger}_{01}(s)\hat{b}_{01}(s)\rangle = \beta_0^2$ we obtain

$$\langle \hat{A}^{\dagger}_1(t)\hat{A}_2(t)\hat{A}^{\dagger}_2(t')\hat{A}_1(t')\rangle = \ g^2\Gamma N_a\beta_0^2\epsilon(t)\epsilon(t')\int_0^t ds\ \epsilon^{-1}(s)\Theta(t' - s). \tag{C11}$$

For $t \geq t'$ we have

$$\langle \hat{A}^{\dagger}_1(t)\hat{A}_2(t)\hat{A}^{\dagger}_2(t')\hat{A}_1(t')\rangle = \ \frac{N_a}{2}\epsilon(t)\left(1 - \epsilon(t')\right), \tag{C12}$$

and using Eq. (C6), (C7) and (C12) we get

$$\langle \hat{N}_{a_1}(t)\hat{N}_{a_1}(t')\rangle = \frac{N_a^2}{4}\epsilon(t)\epsilon(t') + \frac{N_a}{2}\epsilon(t), \tag{C13}$$

while for $t < t'$ we have

$$\langle \hat{A}^{\dagger}_1(t)\hat{A}_2(t)\hat{A}^{\dagger}_2(t')\hat{A}_1(t')\rangle = \ \frac{N_a}{2}\epsilon(t')\left(1 - \epsilon(t)\right), \tag{C14}$$

and

$$\langle \hat{N}_{a_1}(t)\hat{N}_{a_1}(t')\rangle = \frac{N_a^2}{4}\epsilon(t)\epsilon(t') + \frac{N_a}{2}\epsilon(t'). \tag{C15}$$

We notice that we obtain the same result for the double integral with respect to t and t' for both cases, $t \geq t'$ and for $t < t'$

$$\int_0^{\tau}\int_0^{\tau} dt\ dt'\ \langle \hat{N}_{a_1}(t)\hat{N}_{a_1}(t')\rangle = \frac{N_a^2}{4}I_1^2 + \frac{N_a}{2}I_1\tau, \tag{C16}$$

but distinguishing between the two cases would be important when we calculate the covariance of $\hat{J}_z(\tau)$ and $\hat{S}_b(\tau)$. For simplicity, we have also defined

$$I_1(\tau) \equiv \int_0^{\tau} dt\ \epsilon(t) = \frac{1 - \epsilon(\tau)}{2g^2\Gamma\beta_0^2}. \tag{C17}$$

We can now calculate

$$\int_0^{\tau} dt\langle \hat{N}_{a_1}(t)\rangle = \frac{N_a}{2}I_1. \tag{C18}$$

2. Phase Quadrature

In the case of spontaneous emission the photon operator is given by the following equation

$$\hat{b}_1(z_R, t) = \hat{b}_{01}(t)e^{i\frac{g^2}{c}(\Omega + i\Gamma)\hat{a}^{\dagger}_1(t)\hat{a}_1(t)} + \frac{g}{c}\frac{\sqrt{\gamma_3}}{\Delta - i\gamma_3/2}\hat{a}^{\dagger}_1(t)\hat{q}_{1_{\rm in}}(t). \tag{C19}$$

Again, we define the phase quadrature operator of a specific mode of the light field

$$\hat{Y}_1(\tau) = i(\hat{b}_1(\tau) - \hat{b}^{\dagger}_1(\tau)), \tag{C20}$$

where

$$\hat{b}_1(t) = \frac{\sqrt{c}}{\sqrt{\tau}} \int_0^\tau \hat{b}_{01}(t)dt. \tag{C21}$$

Making the small angle approximation $g^2 (\Omega + i\Gamma) \hat{a}_1^\dagger \hat{a}_1 / c << 1$ we obtain

$$\hat{Y}_1 \approx \hat{Y}_{1_{\text{in}}} - \frac{g^2\Omega}{\sqrt{c\tau}} \int_0^\tau \left(\hat{b}_{01}(t) + \hat{b}_{01}^\dagger(t)\right) \hat{a}_1^\dagger(t)\hat{a}_1(t)dt - \frac{g^2\Gamma}{\sqrt{c\tau}} \int_0^\tau \left(\hat{b}_{01}(t) - \hat{b}_{01}^\dagger(t)\right) \hat{a}_1^\dagger(t)\hat{a}_1(t)dt +$$
$$+ i\frac{g\Omega\sqrt{\gamma_3}}{\sqrt{c\tau}} \int_0^\tau dt \left(\hat{q}_{1_{\text{in}}}(t)\hat{a}_1^\dagger(t) - \hat{q}_{1_{\text{in}}}^\dagger(t)\hat{a}_1(t)\right) - i\frac{g\Gamma\sqrt{\gamma_3}}{\sqrt{c\tau}} \int_0^\tau dt \left(\hat{q}_{1_{\text{in}}}(t)\hat{a}_1^\dagger(t) + \hat{q}_{1_{\text{in}}}^\dagger(t)\hat{a}_1(t)\right), \tag{C22}$$

where

$$\hat{Y}_{1_{\text{in}}}(\tau) \equiv i\frac{\sqrt{c}}{\sqrt{\tau}} \int_0^\tau dt \left(\hat{b}_{01}(t) - \hat{b}_{01}^\dagger(t)\right). \tag{C23}$$

We calculate the expectation value of $\hat{Y}_1(\tau)$

$$\langle \hat{Y}_1(\tau) \rangle \approx -\frac{2\beta_0\Omega g^2}{\sqrt{c\tau}} \int_0^\tau dt \langle \hat{N}_{a_1}(t) \rangle. \tag{C24}$$

From Eq. (C18) we get

$$\langle \hat{Y}_1 \rangle^2 \approx \frac{g^4\Omega^2\beta_0^2 N_a^2 I_1^2}{c\tau}. \tag{C25}$$

Now we are going to calculate $\langle \hat{Y}_1^2 \rangle$, where for simplicity we keep only the terms coming from the the first two terms of Eq. (C22), since they are the dominant terms

$$\langle \hat{Y}_1^2 \rangle \approx 1 + \frac{4g^4\Omega^2}{c\tau}\beta_0^2 \int_0^\tau \int_0^\tau dt dt' \langle \hat{N}_{a_1}(t')\hat{N}_{a_1}(t) \rangle. \tag{C26}$$

Substituting Eq. (C16) in (C26) and using (C25) we obtain

$$\text{Var}(\hat{Y}_1(\tau)) \approx 1 + 2\chi_1^2 N_{\text{ph}} N_a \overline{\epsilon(\tau)}, \tag{C27}$$

where we have defined $\chi_1 \equiv \frac{g^2\Omega}{c}$ and $\overline{\epsilon(\tau)} = \frac{1}{\tau}\int_0^\tau \epsilon(t)dt$ which is the time average of the decay. We notice that $\chi_1 = \chi_{\text{ns}}$ in the no spontaneous emission case ($\gamma_3 = 0$). As we mentioned before $\text{Var}(\hat{S}_b) = 2\text{Var}(\hat{Y}_1)$, thus

$$\text{Var}(\hat{S}_b(\tau)) \approx 2 + 4\chi_1^2 N_{\text{ph}} N_a \overline{\epsilon(\tau)}. \tag{C28}$$

3. Covariances

The covariance of $\hat{J}_z$ and $\hat{S}_b$ is again given by $\text{Cov}(\hat{J}_z(\tau), \hat{S}_b(\tau)) = \langle \hat{J}_z(\tau)\hat{Y}_2(\tau) \rangle - \langle \hat{J}_z(\tau)\hat{Y}_1(\tau) \rangle$, which gives

$$\text{Cov}(\hat{J}_z(\tau), \hat{S}_b(\tau)) = \frac{2g^2\Omega\beta_0}{\sqrt{c\tau}} \int_0^\tau dt \left(\langle \hat{N}_{a_1}(\tau)\hat{N}_{a_1}(t) \rangle - \langle \hat{N}_{a_1}(\tau)\hat{N}_{a_2}(t) \rangle\right), \tag{C29}$$

since

$$\langle \hat{N}_{a_1}(\tau)\hat{N}_{a_1}(t) \rangle = \langle \hat{N}_{a_2}(\tau)\hat{N}_{a_2}(t) \rangle \qquad \langle \hat{N}_{a_1}(\tau)\hat{N}_{a_2}(t) \rangle = \langle \hat{N}_{a_2}(\tau)\hat{N}_{a_1}(t) \rangle. \tag{C30}$$

Now we have to be a bit more careful, compared to the no spontaneous emission case, because we have two different expressions for $\langle \hat{N}_{a_1}(t)\hat{N}_{a_1}(t') \rangle$ depending on whether $t \geq t'$ or $t < t'$. That's why we are going to calculate $\text{Cov}(\hat{S}_b(\tau), \hat{J}_z(\tau))$ as well

$$\text{Cov}(\hat{S}_b(\tau), \hat{J}_z(\tau)) = \frac{2g^2\Omega\beta_0}{\sqrt{c\tau}} \int_0^\tau dt \left(\langle \hat{N}_{a_1}(t)\hat{N}_{a_1}(\tau) \rangle - \langle \hat{N}_{a_1}(t)\hat{N}_{a_2}(\tau) \rangle\right). \tag{C31}$$

For the first covariance, where $\tau \geq t$ we use Eq. (C13), hence

$$\int_0^\tau dt\ \langle \hat{N}_{a_1}(\tau)\hat{N}_{a_1}(t)\rangle = \frac{N_a^2}{4}\epsilon(\tau)I_1 + \frac{N_a}{2}\epsilon(\tau)\tau. \tag{C32}$$

We calculate the simpler term

$$\langle \hat{N}_{a_1}(\tau)\hat{N}_{a_2}(t)\rangle = \frac{N_a^2}{4}\epsilon(\tau)\epsilon(t), \tag{C33}$$

since $\hat{a}_1(t)$ commutes with $\hat{a}_2(t')$ for all t and t'. Thus,

$$\int_0^\tau dt\ \langle \hat{N}_{a_1}(\tau)\hat{N}_{a_2}(t)\rangle = \frac{N_a^2}{4}\epsilon(\tau)I_1. \tag{C34}$$

We finally have

$$\mathrm{Cov}(\hat{J}_z(\tau), \hat{S}_b(\tau)) = \chi_1\sqrt{N_{\mathrm{ph}}}N_a\epsilon(\tau), \tag{C35}$$

where we used again $\chi = \frac{g^2\Omega}{c}$. For the second covariance we use Eq. (C15) for $t < t'$ and we obtain

$$\int_0^\tau dt\ \langle \hat{N}_{a_1}(t)\hat{N}_{a_1}(\tau)\rangle = \frac{N_a^2}{4}\epsilon(\tau)I_1 + \frac{N_a}{2}\epsilon(\tau)\tau \tag{C36}$$

$$\int_0^\tau dt\ \langle \hat{N}_{a_1}(t)\hat{N}_{a_2}(\tau)\rangle = \frac{N_a^2}{4}\epsilon(\tau)I_1. \tag{C37}$$

Hence, we finally get the same result for both covariances as we expected

$$\mathrm{Cov}(\hat{J}_z(\tau), \hat{S}_b(\tau)) = \mathrm{Cov}(\hat{S}_b(\tau), \hat{J}_z(\tau) = \chi_1\sqrt{N_{\mathrm{ph}}}N_a\epsilon(\tau). \tag{C38}$$

4. Quantum Enhancement Parameter ξ_s

Substituting Eq. (C28) and (C38) into Eq. (A5) we get

$$\mathrm{Var}(\hat{S}_2(\tau)) \approx \frac{N_a}{4}\epsilon(\tau)\left(1 - \frac{\chi_1^2 N_{\mathrm{ph}}N_a\epsilon(\tau)}{\chi_1^2 N_{\mathrm{ph}}N_a\overline{\epsilon(\tau)} + 1/2}\right). \tag{C39}$$

Using the atomic equations we find the expectation value of $\hat{J}_x$ for $(\chi_1^2 + 2\chi_2)N_{\mathrm{ph}} << 1$

$$\langle \hat{J}_x(t)\rangle \approx \frac{N_a}{2}e^{-(\chi_1^2+2\chi_2)N_{\mathrm{ph}}}, \tag{C40}$$

where we have defined $\chi_2 \equiv g^2\Gamma/c$. Now we can express $\epsilon(\tau)$ in a more convenient way $\epsilon(\tau) = e^{-2\chi_2 N_{\mathrm{ph}}}$. Finally, the squeezing parameter is given by

$$\xi_{s_2} \approx e^{(\chi_1^2+\chi_2)N_{\mathrm{ph}}}\left(1 - \frac{\chi_1^2 N_{\mathrm{ph}}N_a\epsilon(\tau)}{\chi_1^2 N_{\mathrm{ph}}N_a\overline{\epsilon(\tau)} + 1/2}\right)^{1/2}, \tag{C41}$$

where for convenience we present again all the parameter definitions we made throughout this calculation

$$\chi_1 \equiv \frac{g^2\Omega}{c}, \qquad \chi_2 \equiv \frac{g^2\Gamma}{c}, \qquad \overline{\epsilon(\tau)} \equiv \frac{1}{\tau}\int_0^\tau \epsilon(t)dt, \qquad \epsilon(\tau) = e^{-2\chi_2 N_{\mathrm{ph}}}. \tag{C42}$$